Published in final edited form as:

Cell Rep. 2021 September 21; 36(12): 109706. doi:10.1016/j.celrep.2021.109706.

ATF3 promotes the serine synthesis pathway and tumor growth under dietary serine restriction

Xingyao Li[1,7], **Daniel Gracilla**[1,7], **Lun Cai**[1], **Mingyi Zhang**[1,2], **Xiaolin Yu**[1], **Xiaoguang Chen**[2], **Junran Zhang**[3], **Xiaochun Long**[4], **Han-Fei Ding**[1,5], **Chunhong Yan**[1,6,8,*]

[1]Georgia Cancer Center, Augusta University, Augusta, GA 30912, USA

[2]Institute of Materia Medica, Peking Union Medical College, Beijing 100050, China

[3]Department of Radiation Oncology, Ohio State University James Comprehensive Cancer Center and College of Medicine, Columbus, OH 43210, USA

[4]Vascular Biology Center, Medical College of Georgia, Augusta University, Augusta, GA 30912, USA

[5]Department of Pathology, Medical College of Georgia, Augusta University, Augusta, GA 30912, USA

[6]Department of Biochemistry and Molecular Biology, Medical College of Georgia, Augusta University, Augusta, GA 30912, USA

[7]These authors contributed equally

[8]Lead contact

SUMMARY

The serine synthesis pathway (SSP) involving metabolic enzymes phosphoglycerate dehydrogenase (PHGDH), phosphoserine aminotransferase 1 (PSAT1), and phosphoserine phosphatase (PSPH) drives intracellular serine biosynthesis and is indispensable for cancer cells to grow in serine-limiting environments. However, how SSP is regulated is not well understood. Here, we report that activating transcription factor 3 (ATF3) is crucial for transcriptional activation of SSP upon serine deprivation. ATF3 is rapidly induced by serine deprivation via a mechanism dependent on ATF4, which in turn binds to ATF4 and increases the stability of this master regulator of SSP. ATF3 also binds to the enhancers/promoters of *PHGDH*, *PSAT1*, and *PSPH* and recruits p300 to promote expression of these SSP genes. As a result, loss of *ATF3* expression impairs serine biosynthesis and the growth of cancer cells in the serine-deprived medium or in

*Correspondence: cyan@augusta.edu.

AUTHOR CONTRIBUTIONS

Conceptualization, C.Y.; funding acquisition, C.Y. and H.-F.D.; investigation, X.L.(Xingyao Li), D.G., L.C., M.Z., and X.Y.; methodology, H.-F.D., X.L. (Xiaochun Long), J.Z., and X.C.; supervision, X.C., J.Z., X.L.(Xiaochun Long), H.-F.D., and C.Y.; writing, C.Y.

SUPPLEMENTAL INFORMATION

Supplemental information can be found online at https://doi.org/10.1016/j.celrep.2021.109706.

DECLARATION OF INTERESTS

The authors declare no competing interests.

mice fed with a serine/glycine-free diet. Interestingly, *ATF3* expression positively correlates with *PHGDH* expression in a subset of TCGA cancer samples.

Graphical Abstract

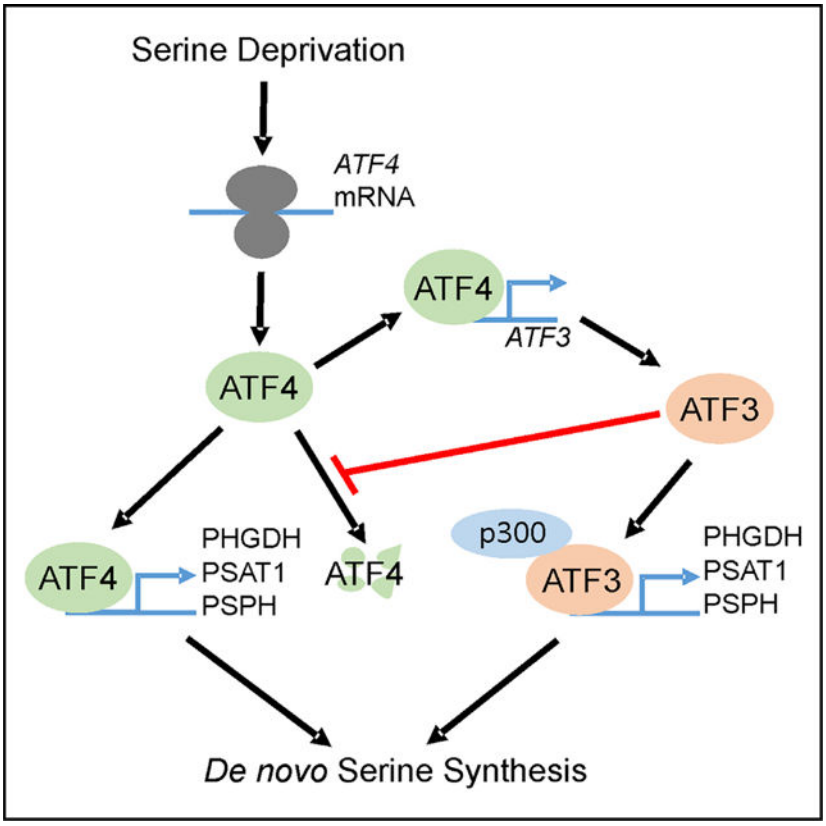

In brief

Activation of the serine synthesis pathway is important for cancer cell growth, but how this pathway is regulated is not well understood. Li et al. report that ATF3 is an important regulator of this pathway and can promote serine biosynthesis and tumor growth under serine-limiting conditions.

INTRODUCTION

As an important amino acid to cells, serine is not only proteinogenic but also required for the biosynthesis of many intracellular molecules, such as sphingolipids, phospholipids, and glutathione (Mattaini et al., 2016). Serine can also be converted into glycine while donating one-carbon units for folate-dependent reactions, yielding thymidine and purine bases for nucleotide synthesis or S-adenosylmethione for DNA/protein methylation (Mattaini et al., 2016; Yang and Vousden, 2016). In addition to importing serine from the extracellular environment, cells can synthesize serine from the glycolytic intermediate 3-phosphoglycerate (3-PG) through 3 consecutive reactions catalyzed by phosphoglycerate dehydrogenase (PHGDH), phosphoserine aminotransferase (PSAT), and phosphoserine

phosphatase (PSPH), respectively—a process collectively referred to as the serine synthesis pathway (SSP) (Mattaini et al., 2016). Although serine is one of the most consumed amino acids in cultured cells, increased serine biosynthesis is one of many metabolic changes found in cancer and has been shown to be required for rapid tumor growth (Sullivan et al., 2019). Indeed, while PHGDH, the rate-limiting enzyme in SSP, is often overexpressed in human cancer (Li and Ye, 2020), serine deprivation from the extracellular environment by dietary restriction of serine, or direct blockage of serine biosynthesis via pharmacological inhibition of PHGDH, can inhibit tumor growth and limit metastatic spreads of cancer cells into mouse brains (Maddocks et al., 2013; Ngo et al., 2020; Xia et al., 2019). Hence, targeting SSP or serine biosynthesis has emerged as a promising strategy for therapeutic intervention of cancer.

Although high *PHGDH* expression can be caused by gene amplification or a defect in Parkin-mediated protein degradation (Liu et al., 2020; Possemato et al., 2011), how SSP and serine biosynthesis are regulated in cancer is not well understood. Transcriptional regulation of the expression of genes encoding the 3 SSP enzymes, i.e., PHGDH, PSAT1, and PSPH, appears to be a major mechanism for the regulation of serine biosynthesis (Li and Ye, 2020). Indeed, the promoters/enhancers of SSP genes contain binding sites for several transcription factors, including activating transcription factor 4 (ATF4) and c-Myc. Expression of ATF4, a member of the ATF/CREB family of transcription factors, can be induced by various cellular stresses (e.g., serine deprivation) through activation of eIF2α, which specifically enhances translation of *ATF4* mRNA (Wortel et al., 2017). ATF4 can bind to SSP genes and transactivate their expression to enhance serine biosynthesis and sustain rapid growth of cancer cells under serine-deprived conditions (DeNicola et al., 2015; Ye et al., 2012). In line with the important role that SSP plays in the regulation of serine metabolism, knockdown of *ATF4* expression largely impairs the growth of cancer cells cultured in serine-deprived media (Ye et al., 2012). Interestingly, while the major antioxidant transcription factor Nrf2 transcriptionally induces ATF4 to activate *PHGDH* and *PSAT1* expression in non-small cell lung cancers (DeNicola et al., 2015), KDM4C, a histone H3 lysine 9 demethylase, as well as the transcription factor MYCN, promote transcription of SSP genes in neuroblastoma cells in an ATF4-dependent manner (Xia et al., 2019; Zhao et al., 2016a). Thus, ATF4 appears to be the master transcriptional regulator for the serine synthesis pathway and could be targeted for the treatment of cancer (Yang and Vousden, 2016). However, as *Atf4* null mice exhibit developmental defects (Masuoka and Townes, 2002), direct ATF4 targeting may result in severe undesired effects. It thus remains crucial to identify genes that play important roles in the regulation of the serine synthesis pathway.

Here, we report that the ATF3, an ATF4 family member, is another protein central to the regulation of the serine synthesis pathway and tumor growth under serine-limiting conditions. Like ATF4, ATF3 induced by various cellular stresses (e.g., nutrient deprivation, endoplasmic reticulum stress, and oxidative stress) can regulate transcription of genes involved in stress signaling (Hai and Hartman, 2001; Wortel et al., 2017). However, ATF3 is distinct from ATF4 and only contains a functional domain (i.e., the basic region leucine zipper [bZIP]) structurally similar to that of ATF4. ATF3 can interact with many other proteins (e.g., p53, nuclear factor κB [NF-κB], and HDAC1/3) and thus exhibits distinct biological functions, such as the regulation of cellular response to DNA damage

or immunogenic stimuli (Gilchrist et al., 2006; Nguyen et al., 2020; Yan et al., 2005). In this report, we demonstrate that ATF3 induced by serine deprivation promoted the serine synthesis pathway by increasing the ATF4 stability while recruiting the transcriptional co-activator p300 to transactivate SSP genes.

RESULTS

ATF3 is induced by serine deprivation in an ATF4-dependent manner

Although cells can divert up to 10% of glycolytic carbon to serine biosynthesis to support proliferation (Mattaini et al., 2016), deprivation of serine from the extracellular environment can activate the serine synthesis pathway by inducing expression of transcription factors like ATF4 via activation of GCN2 and eIF2α (Ye et al., 2012). As ATF3 is a common stress sensor, we sought to determine whether *ATF3* expression can also be induced by the metabolic stress caused by serine deprivation. We thus incubated various cells, including immortalized hTERT-RPE1 epithelial cells (RPE in short), U2OS sarcoma cells, PC3 prostate cancer cells, and HCT116 colon cancer cells, in a culture medium deprived of serine and glycine and determined *ATF3* expression by western blotting and qRT-PCR assays. The reason why we also depleted glycine from the culture medium was that imported glycine can be converted to serine, thereby bypassing the serine synthesis pathway (Locasale, 2013). Not surprisingly, serine deprivation caused a dramatic increase in both the protein (Figure 1A) and the mRNA level (Figures 1B and 1C) of *ATF3*, suggesting that serine deprivation likely induced *ATF3* expression at the transcription level. Although *ATF3* induction was an immediate early event (Figure 1D) and the kinetics of ATF3 induction by serine deprivation varied among cell lines, the *ATF3* expression level was decreased to the basal level 48 h after serine deprivation (Figures 1A–1C). The latter results were not unexpected, as ATF3 can bind to and repress its own promoter (Wolfgang et al., 2000; Zhao et al., 2016b). Interestingly, although the conversion between serine and glycine is bidirectional (Locasale, 2013), deprivation of only serine from the culture medium was sufficient to induce *ATF3* expression while deprivation of glycine only slightly induced *ATF3* expression (Figure 1E), in line with the notion that the glycine to serine conversion is not sustainable (Ding et al., 2013). As a transient increase of *ATF4* expression is the major molecular event in response to serine deprivation, we determined whether ATF3 induction was mediated by ATF4. In line with previous findings that the *ATF3* promoter contains a C/EBP-ATF response element (CARE) (5′-TGATGCAA-3′; −23 to −16) that can be bound by ATF4 and is responsible for *ATF3* induction (Jiang et al., 2004; Pan et al., 2003; Wolfgang et al., 2000), knockdown of *ATF4* expression using a previously characterized *ATF4* short hairpin RNA (shRNA) (Zhao et al., 2016a) almost completely diminished *ATF3* induction by serine deprivation (Figure 1F)—results unlikely from off-target activities of the *ATF4* shRNA as *ATF3* induction by serine deprivation was abolished in *ATF4*-knockout (KO) HEK293T cells as well (Park et al., 2017; Figure 1G). These results argue for a notion that serine deprivation induced *ATF3* expression through a mechanism involving the GCN2-eIF2α-ATF4 axis. In support of this notion, NCT-503, a PHGDH inhibitor (Pacold et al., 2016) that can inhibit serine biosynthesis but unlikely activate this axis, failed to induce *ATF3* expression (Figure S1).

ATF3 is required for cell growth under serine-deprived conditions

Deprivation of serine from the extracellular environment can impair cell growth (Maddocks et al., 2013; Ye et al., 2012). Because serine deprivation profoundly induced *ATF3* expression, we determined whether ATF3 is required for cell growth under serine-deprived conditions. Although serine deprivation indeed slowed cell growth, KO of *ATF3* expression in various cells (Figure 2A) significantly impaired the growth of these cells in the serine-deprived (Ser(−)) medium but did not, or only marginally, affect their growth in the complete (Ser(+)) medium (Figures 2B–2E, S2A, and S2B). The growth defects were unlikely caused by CRISPR-Cas9-mediated off-target editing, as we observed similar effects in *ATF3*-KO HCT116 cells previously engineered using a distinct, AAV (Adeno-associated virus)-based, precise genome-editing approach (Zhao et al., 2016b; Figure 2F). These results thus argue that ATF3 induction is crucial for sustaining cancer cell growth under serine-deprived conditions. Although p53 can regulate cancer cell growth in the serine-deprived medium (Maddocks et al., 2013) and ATF3 can activate p53 in the DNA damage response (Li et al., 2020; Yan et al., 2005), it is noteworthy that ATF3 unlikely promoted cancer cell growth through activating p53 as PC3 cells are p53 null and DU145 cells carry a mutant p53 gene. Moreover, loss of *ATF3* expression impaired the growth of p53-deficient HCT116 cells in the serine-deprived medium as well (Figures S2C and S2D).

ATF3 supports tumor growth under dietary serine restriction

Dietary restriction of serine can slow tumor growth in mice (Labuschagne et al., 2014; Maddocks et al., 2013). To determine whether ATF3 also supports *in vivo* tumor growth in serine-restricted conditions, we implanted ATF3-wild-type (WT) and KO HCT116 cells (Figure 2F) into nude mice fed with a diet deprived of both serine and glycine (SG(−)) or with a control complete diet (SG(+)). As previously reported (Maddocks et al., 2013), dietary restriction of serine significantly inhibited the growth of HCT116 xenografts (Figures 2G–2I) but did not cause overt toxicity to mice because the mouse weight was not changed (Figure S2E). Importantly, although ATF3 did not appear to affect tumor growth in mice fed with the complete diet, *ATF3*-KO cells grew significantly slower than the WT cells when the mice were fed with the serine-deprived diet (Figures 2G–2I). Staining of the tumor sections for expression of the proliferation marker Ki67 confirmed that serine deprivation decreased the proliferation rate of cancer cells, while this rate was further decreased in *ATF3*-deficient cells (Figures 2J and 2K). These results thus demonstrate that *ATF3* induction is required for tumor growth under dietary serine restriction.

ATF3 regulates the serine synthesis pathway and serine biosynthesis

To answer the question as to how ATF3 supports cancer cell growth under serine-deprived conditions, we subjected ATF3-WT and KO cells to RNA sequencing (RNA-seq) analyses. Serine deprivation induced expression of 609 genes while downregulating expression of 454 genes (Figure S3A; Table S1). The most enriched gene set induced by serine deprivation was that for the serine biosynthesis process, followed by the gene set involved in amino acid transport. Serine deprivation also significantly induced expression of *ATF4* and its known targets, including *ATF3*, *ASNS*, and *DDIT3*—genes known to engage in the endoplasmic reticulum (ER) stress response (Figure S3B). Out of these genes, ATF3 appeared to be

required for inducing 61 genes and repressing 23 genes (Figure 3B; Table S2), which include several genes (e.g., *DDIT3*, *CHAC1*, and *GDF15*) previously shown to be ATF3 transcriptional targets (Crawford et al., 2015; Lee et al., 2010; Wang et al., 2020; Wolfgang et al., 1997) and genes encoding amino acid transporters (e.g., *SLC1A4*; Figure 3B). Importantly, although the gene set for serine biosynthetic process remained as the most enriched GO (Gene Ontology) term (Figure 3C), ATF3 regulated expression of all 3 genes (i.e., *PHGDH*, *PSAT1*, and *PSPH*) encoding the serine synthetic enzymes (Figures 3A and 3C). These unbiased data suggest that ATF3 likely promoted expression of SSP genes, thereby promoting serine biosynthesis to support cancer cell growth. Indeed, while serine deprivation caused rapid increases in the *PHGDH*, *PSAT1*, and *PSPH* mRNA levels in various cells, loss of *ATF3* expression profoundly impaired the induction of all 3 SSP genes (Figure 3D). Moreover, serine-deprivation-induced increases in the PHGDH and PSAT1 protein levels were suppressed by *ATF3* deficiency (Figure 3E). Note that ATF3 exhibited same effects in p53-null PC3 cells (Figures 3D and 3E), suggesting that these effects were likely p53 independent. To determine whether ATF3 regulates serine biosynthesis, we incubated the isogenic HCT116 cells differing in *ATF3* expression in a medium containing [U-^{13}C]-glucose for stable isotope tracing assays. While serine deprivation caused a dramatic increase in newly synthesized serine labeled with [^{13}C] (the M+3 fraction), loss of ATF3 significantly suppressed serine synthesis induced by serine deprivation (Figure 3F). These results thus argue that ATF3 can promote cancer cell growth under serine-limiting conditions by inducing SSP gene expression and promoting serine biosynthesis.

ATF3 binds to ATF4 to increase the stability of the latter protein

ATF4 is the master transcriptional activator for SSP genes (DeNicola et al., 2015; Ye et al., 2012). Intriguingly, ATF4 induction by serine deprivation was dramatically diminished in the *ATF3*-deficient cells (Figure 4A). Mainly regulated at the post-transcriptional level (Kilberg et al., 2009), ATF4 was an unstable protein with a half-life of ~20 min (Figures 4B and 4C). Although loss of ATF3 did not appear to alter the *ATF4* mRNA level (Figure S4A), the half-life of ATF4 induced by serine deprivation was reduced to ~10 min in the *ATF3*-deficient cells (Figures 4B and 4C), suggesting that ATF3 induced by serine starvation likely in turn stabilized ATF4. In line with this notion, transient co-expression of ATF3 increased the ATF4 level (Figure 4D) as a result of increased half-life (Figures 4E and 4F). These results are reminiscent of our previous findings that ATF3 can stabilize other proteins by binding to them (e.g., p53 and Tip60; Cui et al., 2015; Yan et al., 2005). Indeed, we confirmed an earlier observation that ATF3 bound to ATF4 (Figures 4G, 4H, and S4B; Wang et al., 2009). Moreover, although deleting the ATF3 leucine-zipper domain (ZIP) appeared to diminish this interaction (Figures 4G, 4H, and S4B), an ATF3 mutant lacking ZIP (ΔZIP) failed to increase the ATF4 level (Figure 4D) or its half-life (Figures 4E and 4F), suggesting that the ATF3-ATF4 interaction was required for ATF4 stabilization. We concluded that ATF3 induced by serine deprivation likely bound to ATF4 to increase its stability, thereby promoting SSP gene expression and serine biosynthesis via a positive feedback loop.

ATF3 binds to the promoter/enhancer regions of SSP genes and regulates their expression

ATF3 is a DNA binding protein and can bind to the ATF/CREB (5′-TGACGTCA-3′), AP-1 (5′-TGAC/GTCA-3′), or CARE (5′-TGATGCAA-3′) *cis*-regulatory element (Zhao et al.,

2016b). Interestingly, we re-analyzed our published ATF3 chromatin immunoprecipitation sequencing (ChIP-seq) data (GEO: GSE74363; Zhao et al., 2016b) and found that ATF3 had a very strong binding peak (hg19 chr1: 120,255,339–120,255,465) in the first intron of the *PHGDH* gene (Figures 5A and S5A), which overlapped with an ATF4-binding peak revealed by ENCODE (Encyclopedia of DNA Elements) (Figure 5A). The center of the peak contained a CARE site (5′-TGATGCAA-3′; Figure 5A) previously shown to be bound by ATF4 in A549 lung cancer cells (DeNicola et al., 2015). This earlier study also suggests that the intron 1 of *PSAT1* contains a reverse CARE element (5′-TTGCATCA-3′; +249 to +257) that could be bound by ATF4 (DeNicola et al., 2015). However, ATF3 did not appear to bind to this element but rather bind to a region (hg19 chr9: 80,912,032–80,912,156) close to the *PSAT1* transcription start site and overlapping with an ENCODE ATF4 peak (Figures 5B and S5B). This region contained an AP-1 element (5′-TGACTCA-3′; Figure 5B). On the other hand, ATF3 bound strongly to a genomic region located in the *PSPH* intron 2 (hg19 chr7: 56,101,365–56,101,489) and containing a reverse CARE site (Figure S5C), while two inducible ATF3-binding peaks flanked the transcription start site of *PSPH* (Figure 5C). The intron 1 peak (hg19 chr7: 56,118,214–56,118,338) contained an AP-1 site (5′-TGAGTCA-3′) and overlapped with an ENCODE ATF4 peak, although the promoter peak (chr7: 56,119,250–56,119,374) contained a CARE-like site (5′-TGATCAA-3′). We carried out ChIP-qPCR assays to determine whether ATF3 binds to these genomic regions in response to serine deprivation. Indeed, although the ATF3 antibody could pull down DNA fragments corresponding to these regions (Figures 5D–5F), serine deprivation dramatically increased the amount of bound ATF3 (Figures 5D–5F), suggesting that the metabolic stress induced by serine starvation promoted ATF3 to bind to SSP genes. As the ATF3 antibody did not pull down a non-specific DNA fragment localized in the *PHGDH* intron 4 (Figure 5G; marked as NS in Figure S5A) or precipitate DNA from the *ATF3*-KO cells (Figure 5H), it was unlikely that the detected ATF3 binding to these SSP gene regions was due to non-specific antibody binding. These results thus indicate that ATF3 also bound to SSP genes upon serine deprivation.

As the strong ATF3-binding peak in *PHGDH* intron 1 was flanked by chromatins enriched with K27-acetylated H3 (H3K27ac) (Figures 5A and S5D) and H3K27ac is a marker for active enhancers (Calo and Wysocka, 2013; Creyghton et al., 2010), we cloned this region into a pGL4 vector containing a minimal promoter (MiniP) (Figure 5I) for reporter assays. Indeed, this small DNA fragment (~250 bp) dramatically enhanced the activity of MiniP to drive *luc2* expression (Figure 5I), supporting that this ATF3-bound fragment was an active enhancer that could promote *PHGDH* expression. However, transient overexpression of ATF3 or ATF4 only slightly altered the activity of the *PHGDH* enhancer (Figure 5I), probably because not only an ATF family member (e.g., ATF3 or ATF4) but also a C/EBP transcription factor were required to be overexpressed and bind the CARE (C/EBP-ATF) composite site (Figure 5A) to activate transcription (Kilberg et al., 2009). Serine starvation could induce expression of C/EBP genes (e.g., *CEBPB* and *CEBPG*; Figure 3B) through ATF4 (Thiaville et al., 2008), and these C/EBP factors might subsequently bind to the CARE site along with ATF3 or ATF4 to enhance *PHGDH* expression. In line with this notion, ectopically expressed ATF3 failed to promote *PHGDH* and *PSAT1* expression

induced by serine deprivation in the *ATF4*-KO HEK293T cells but could do so in the *ATF4*-competent cells (Figures 5J and 5K).

ATF3 recruits p300 to the promoter/enhancer of PHGDH and PSAT1

p300 is one of the best-characterized transcriptional co-activators that can "bridge" transcription factors to the basal transcription machinery while modifying the chromatin environment (Wang et al., 2013). Previously, we found that 37% of p300-binding peaks overlap with ATF3-binding peaks on the genome level (Zhao et al., 2016b), suggesting that ATF3 may recruit p300 to genomic sites for transcriptional activation. Interestingly, p300 also appeared to regulate the serine synthesis pathway as the p300 inhibitor C646 (Bowers et al., 2010) inhibited SSP gene expression upon serine deprivation (Figure S6A), while the growth of p300-KO (p300KO) HCT116 cells was impaired in the serine-deprived medium (Figure S6B). We therefore tested a possibility that ATF3 recruits p300 to the promoters/enhancers of SSP genes to activate their expression. First, we carried out coimmunoprecipitation (coIP) assays and found that a FLAG antibody could co-precipitate ATF3 only in the presence of FLAG-tagged p300 (Figure 6A) and that a p300 antibody could pull down the endogenous ATF3 from cell lysates (Figure 6B). Using a cell line engineered to conjugate a 3× FLAG to the C terminus of the endogenous ATF3 protein, we found that the FLAG antibody could pull down endogenous p300 along with the tagged ATF3 (Figure 6C). Thus, ATF3 could bind to p300 *in vivo*. Moreover, as immobilized glutathione S-transferase (GST)-ATF3 pulled down the purified p300 protein in a GST-pull-down assay (Figure 6D), ATF3 appeared to directly bind to p300. Next, we carried out ChIP assays to determine whether loss of *ATF3* expression affects p300 recruitments to SSP genes. p300 bound to the *PHGDH*/*PSAT1* enhancer/promoter regions where ATF3 bound to, and serine deprivation promoted p300 to bind to these regions (Figures 6E and 6F). Importantly, the amounts of p300 bound to the *PHGDH* enhancer (Figure 6E) or the *PSAT1* promoter (Figure 6F) were significantly decreased in *ATF3*-KO cells, in line with the notion that ATF3 is required for p300 recruitments to SSP genes upon serine deprivation. To test whether the p300 recruitment is required for ATF3-mediated induction of SSP gene expression, we knocked out p300 expression from *ATF3*-WT and KO HCT116 cells (Figure 6G). Although *ATF3* deficiency again impaired serine-deprivation-induced *PHGDH* and *PSAT1* expression in p300-WT cells, such effects were largely compromised in absence of p300 (Figures 6H and 6I). Similar results were obtained when the p300 activity was inhibited by a specific inhibitor A485 (Lasko et al., 2017; Figures S6E and S6F), suggesting that the p300 catalytic activity was required for ATF3-mediated regulation. These results thus support a notion that ATF3 recruits p300 to SSP genes to transcriptionally activate the serine synthesis pathway.

ATF3 expression correlates with PHGDH expression in human cancer

PHGDH encodes the rate-limiting enzyme for serine biosynthesis, and thus its overexpression in cancer can promote serine metabolism and support cancer growth (Li and Ye, 2020; Ngo et al., 2020; Possemato et al., 2011; Sullivan et al., 2019). However, how *PHGDH* expression is regulated in cancer is not well understood. In TCGA (The Cancer Genome Atlas) PanCancer Atlas Studies, *PHGDH* amplification was found in several types of human cancer (Figure 7A). Although higher *PHGDH* copy numbers correlated with

higher mRNA levels (Figure 7B), the overall *PHGDH* amplification frequency was only 1.05% (Figure 7A), suggesting that a mechanism other than copy number variations might be responsible for the regulation of *PHGDH* expression in cancer. Because ATF3 could bind to the *PHGDH* enhancer and regulate its expression (Figure 5), we explored a possibility that ATF3 also contributes to the regulation of basal *PHGDH* expression in cancer. We thus retrieved *ATF3* and *PHGDH* expression data from the TCGA PanCancer Studies for correlation analysis. Indeed, *ATF3* expression positively correlated with *PHGDH* expression in several types of cancer, including testicular germ cell tumors (GCTs), adrenocortical carcinoma, breast-invasive carcinoma, and head and neck squamous cell carcinoma (Figure 7C; $p < 0.01$). The correlation was particularly significant in GCTs (Figure 7C), a rare type of tumors that can be divided into nonseminomatous GCTs (NSGCTs) and seminomas. Interestingly, while NSGCTs grow and spread faster than seminomas, the *PHGDH* expression level was higher in NSGCT than that in seminomas (Figure 7D). As *ATF3* was also highly expressed in NSGCT (Figure 7E), ATF3 might enhance *PHGDH* expression and promote serine biosynthesis, thereby contributing to the fast growth of this subtype of tumors. Note that no *PHGDH* amplification was found in testicular GCTs and adrenocortical carcinoma (Figure 7A). Moreover, although *ATF4* expression also positively correlated with *PHGDH* expression (Table S3), such correlations appeared to be weaker than the correlations between ATF3 and PHGDH in these two types of tumors. The finding that the *ATF3* expression level significantly correlates with that of *PHGDH* in breast cancer was also intriguing, as previous studies indicated that *PHGDH* expression and serine metabolism contribute to breast cancer progression (Possemato et al., 2011) and that *ATF3* is frequently amplified in breast cancer and thought to promote breast cancer progression (Wolford et al., 2013; Yin et al., 2008). Indeed, *ATF3* was amplified in 7.64% of TCGA breast cancer samples (Figure S7A). However, neither *ATF3* amplification nor copy number gains contributed to high *ATF3* expression level (Figures S7B and S7C). These results thus suggest a strong possibility that *ATF3* expression contributes to *PHGDH* overexpression, thereby promoting serine biosynthesis and cancer progression in a subset of cancers.

DISCUSSION

Although cells can obtain serine from the extracellular environment, the serine synthesis pathway remains crucial for sustaining rapid growth of cancer cells (Sullivan et al., 2019). Previously, ATF4 has been identified as the master transcription factor that directly binds to SSP genes to transactivate their expression in response to serine deprivation or oncogenic stress (e.g., Nrf2/MYCN expression; DeNicola et al., 2015; Xia et al., 2019; Ye et al., 2012; Zhao et al., 2016a). In this report, we presented data arguing for a notion that ATF3 is another crucial protein that can transactivate SSP genes and consequently promote serine biosynthesis and tumor growth under serine-restricted conditions. Our results support a model whereby ATF3 induced by ATF4 in turn binds to ATF4 to promote its activation, while ATF3 also recruits p300 to SSP genes for their transactivation (Figure 6J). Indeed, KO of *ATF3* expression largely impaired expression of SSP genes upon serine deprivation (Figure 3) and suppressed serine biosynthesis and cancer growth under serine-deprived conditions (Figure 2). Given that ATF4 is an unstable protein and its induction is a transient event (Kilberg et al., 2009), ATF4-mediated induction of ATF3 could not only

directly transactivate SSP genes but also stabilize ATF4 and thereby might serve as a positive feedback and fail-proof mechanism to ensure transcriptional activation of the serine biosynthesis pathway when the extracellular serine supply is limited or exhausted. This mechanism is distinct from the ATF4 self-limiting model whereby ATF3 induced by histidine deprivation rather antagonizes ATF4, thereby repressing expression of the asparagine synthetase (*ASNS*) gene (Kilberg et al., 2009). Although transcription of SSP genes might be regulated differently from *ASNS* expression, it is noteworthy that the ATF4 self-limiting model was primarily based on transient *ASNS* promoter-reporter assays (Pan et al., 2003). While transient ATF3 expression indeed caused a slight decrease in the *PHGDH* enhancer activity (Figure 5I), it can increase the activity of a promoter containing ATF3-binding sites in other reporter assays (Li et al., 2020; Liu et al., 2011). In light of the facts that cancer growth as well as brain metastasis are dependent on serine biosynthesis (Ngo et al., 2020; Sullivan et al., 2019; Xia et al., 2019) and that *ATF4* deficiency may cause severe side effects (Masuoka and Townes, 2002), our results support an anti-cancer strategy centered on targeting the ATF3-mediated regulation of serine biosynthesis. This strategy is further supported by the observations that ATF3 likely contributes to *PHGDH* expression in a subset of cancers (Figure 7).

While ATF3 can repress transcription by either displacing transcription activators or recruiting transcriptional co-repressors (e.g., histone deacetylases; Gilchrist et al., 2006; Nguyen et al., 2020; Wang et al., 2020), the mechanism(s) by which ATF3 increases transcriptional activity is not well understood. ATF3 can form dimers with other bZIP-containing proteins, such as other ATF/CREB members (Rodríguez-Martínez et al., 2017). It is proposed that ATF3 homodimers repress while ATF3 heterodimers transactivate transcription (Hai and Hartman, 2001). Consistent with an early report (Wang et al., 2009), although ATF3 could bind to ATF4, transient co-expression of ATF4 with ATF3 did not enhance *PHGDH* expression (data not shown). Rather, we found that ATF3 could bind to p300 and recruit p300 to SSP genes to enhance their expression (Figure 6). As up to 37% of p300-enriched genomic regions were also bound by ATF3 (Zhao et al., 2016b), ATF3-mediated recruitment of p300 to genomic sites could serve as a general mechanism utilized by ATF3 to enhance transcription. These results also suggest that p300 likely plays an important role in the regulation of serine synthesis pathway. Indeed, p300 inhibition impaired SSP expression induced by serine starvation (Figure S6A). Interestingly, an early study found that p300 can also interact with ATF4 and increase its stability (Lassot et al., 2005). However, although ATF4 might similarly recruit p300 to SSP genes, we did not find that p300 increased the ATF4 level under serine-deprived conditions (Figures S6F and S6G). As loss of p300 did not completely abolish SSP expression induced by serine deprivation (Figures 6H and 6I), other transcriptional co-activators might involve in the regulation of SSP transcription as well. Indeed, ATF3 appeared to bind to the p300 paralog CBP as well (data not shown).

It has been shown that the tumor suppressor p53 regulates cancer growth under serine-deprived conditions by inducing p21 expression (Maddocks et al., 2013). Surprisingly, p53 can repress *PHGDH* expression by binding to a putative site (−606 to −633) in the human *PHGDH* promoter when its expression was induced by nutlin-3 or DNA-damaging agents (Ou et al., 2015). Although we previously showed that ATF3 can activate p53 by

increasing its stability (Yan et al., 2005), ATF3 rather promoted *PHGDH* expression (Figures 5J and 5K) and regulated cancer growth under serine-deprived conditions independent of p53 (Figure S1D). These results are not unexpected as serine deprivation only marginally increases the p53 level (Maddocks et al., 2013; Ou et al., 2015), and ATF3 regulates the p53 stability mainly through competing with p53 for MDM2-mediated ubiquitination (Li et al., 2020). As a major p53-negative regulator, MDM2 was recently shown to regulate SSP gene expression through binding to chromatin—a mechanism independent of p53 (Riscal et al., 2016). While the recruitment of MDM2 to chromatin appears to require an interaction with ATF3, or ATF4 (Riscal et al., 2016), how chromatin-bound MDM2 enhances SSP gene expression remains elusive. This recent finding thus links ATF3 and ATF4 expression induced by serine deprivation to an oncogenic function of MDM2 that is independent of its regulation of p53 and suggests an additional mechanism by which ATF3 or ATF4 regulates the serine synthesis pathway. As ATF3 strongly binds to MDM2 (Li et al., 2020; Mo et al., 2010), targeting ATF3 might dissociate MDM2 from chromatin, leading to further inhibition of serine biosynthesis as well as the inhibition of other oncogenic activities of MDM2.

However, it is noteworthy that ATF3 appears to play dual roles in tumorigenesis. Although ATF3 has been shown to promote breast cancer metastasis and cyclosporine-A-induced squamous cell carcinoma of the skin (Wu et al., 2010; Yin et al., 2008), ATF3 also exhibits a tumor-suppressor activity in glioblastoma, as well as colon, lung, and bladder cancers (Gargiulo et al., 2013; Hackl et al., 2010; Jan et al., 2012; Yuan et al., 2013). Indeed, genetic studies indicate that *Atf3* deficiency in mice not only promotes genomic instability and spontaneous tumorigenesis (Wang et al., 2018) but also accelerates prostate tumorigenesis induced by sex hormones or loss of the tumor suppressor Pten (Wang et al., 2015, 2016). Interestingly, although *ATF3* deletions or loss-of-function mutations are frequently noted in human cancer samples (Li et al., 2020), *ATF3* amplifications are also found in subtypes of cancer, e.g., breast and liver cancer (Figure S5). Similarly, *ATF3* expression appears to be upregulated in some cancer types while being downregulated in others (Wang and Yan, 2015; Yan and Boyd, 2006). Our current finding that ATF3 promoted the serine synthesis pathway thus warrants further investigations into the oncogenic activity of ATF3 in serine-restrictive environments, such as metastasis in the brain (Ngo et al., 2020). On the other hand, ATF3 has established roles in the regulation of innate immunity (Gilchrist et al., 2006; Whitmore et al., 2007). Whether therapeutic induction of ATF3 might repress anti-cancer immune responses thereby promoting tumor survival also warrants further investigations.

During the revision of this work, a report was published showing that knockdown of *ATF3* expression decreases basal SSP gene expression and impairs serine biosynthesis in leukemia cells where *ATF3* expression is upregulated (Di Marcantonio et al., 2021). While ATF3 as a common stress sensor frequently expresses at a very low basal level and is often not required for cell proliferation under basal conditions (Hai et al., 1999; Yan and Boyd, 2006), our findings that ATF3 not only bound to SSP genes but also promoted ATF4 activation upon serine deprivation unveil a more general role that ATF3 plays in the regulation of cellular metabolism. Together with our work, the recently published study supports that ATF3 is an important regulator of the serine synthesis pathway.

STAR★METHODS

RESOURCE AVAILABILITY

Lead contact—Further information and requests for resources and reagents should be directed to and will be fulfilled by the lead contact, Chunhong Yan (cyan@augusta.edu).

Materials availability—Cell lines and plasmids generated in this study are preserved by Dr. Chunhong Yan's laboratory and are available upon request.

Data and code availability

- The RNA-seq data and metabolomics data generated in this study have been deposited at the NCBI GEO database (access number: GSE164850) and National Metabolomics Data Repository (Project ID: PR001203; https://doi.org/10.21228/M86Q68), respectively, and are publicly available as of the date of this publication.
- This paper does not report original code.
- Any additional information required to reanalyze the data reported in this paper is available from the lead contact upon request.

EXPERIMENTAL MODEL AND SUBJECT DETAILS

Mice—Animal experiments were carried out in strict accordance with the guidelines of the Institutional Animal Care and Use Committee (IACUC) at the Augusta University. The protocol was approved by the IACUC at the Augusta University (#2013–0584). Male athymic nude mice (Hsd:Athymic Nude-Foxn1^{nu}) purchased from Envigo were used in this study. They were housed in a pathogen-free, barrier facility, and implanted with tumor cells at ~6 weeks of age. They were fed with a diet free of serine and glycine, or a control normal diet, until the completion of the experiments, as described below.

Cell lines—hTERT-RPE1, U2OS, DU145, and 293T cells were routinely cultured in DMEM. HCT116 cells were initially cultured in McCoy's5A medium, but cultured in DMEM for at least 1 month before serine starvation. LNCaP and PC3 cells initially cultured in RPMI medium were similarly cultured to DMEM. All these media were supplemented with 10% of FBS. For serine starvation, cells were first cultured in MEM (GIBCO) supplemented with 10% of dialyzed FBS (GIBCO), 1 × Vitamin Solution (GIBCO), 100 μM of sodium pyruvate, 0.4 mM of serine, and 7.5 mg/L of glycine (the complete medium, or Ser(+)) for 2 days, washed with PBS for 2 times, and then cultured in MEM supplemented with FBS, vitamins, and sodium pyruvate, but without addition of serine and glycine (the serine-deprived medium, or Ser(−)), for different time.

METHOD DETAILS

Generation of knockout cells with CRISPR/Cas9—The CRISPR-Cas9 system was used to generate *ATF3*- and *EP300*-knockout cells as described (Ran et al., 2013). Briefly, a single guided RNA (sgRNA) targeting a region spanning the *ATF3* start codon (5′-AAAATGATGCTTCAACACCCAGG-3′; the start codon was underlined), or a region

immediately downstream of the *EP300* start codon (5′-GAGAATGTGGTGGAACCG-3′), was cloned into pSpCas9(BB)-2A-puro, and used to transfect cells. After selection with puromycin (1–2 μg/ml) for two days, single viable cells were seeded into 96-well plates. Derived single clones were then subjected to western blotting to screen for loss of *ATF3* or p300 expression. A second round of genome editing was performed if gene expression was not completely lost.

Western blotting and quantitative reverse transcription-PCR (qRT-PCR)—These were carried out as described previously (Wang et al., 2020; Yan et al., 2005). For western blotting, cells were lysed in RIPA buffer (50 mM Tris-HCl, pH7.4, 150 mM NaCl, 1% NP-40. 0.1% SDS, 0.5% sodium deoxycholate, 1 mM EDTA) supplemented with proteinase inhibitor cocktails (PI78430, Fisher Scientific). The following antibodies were used: ATF3 (sc-188X, 1:10,000), ATF4 (sc-200, 1:1,000), p300 (sc-584, 1:200), and p53 (sc-126, 1:1000) from Santa Cruz; PHGDH (HPA021241, 1:300), β-actin (A2228, 1:10,000) from Sigma-Aldrich; and PSAT1 (21020002, 1:3,000) from Novus. For qRT-PCR, total RNA was isolated using TRIzol (Invitrogen), following by reverse transcription using 1 μg of total RNA and the iScript Adv cDNA synthesis kit (Bio-Rad). cDNAs were subjected to real-time PCR using SYBR Green (Bimaker) and the StepOnePlus Real-time PCR System (Applied Biosystems). The primers are listed in Table S4.

Co-immunoprecipitation (co-IP) and GST-pulldown assays—For co-IP assays, HEK293T cells transfected with indicated plasmids for two days were lysed in cold FLAG lysis buffer (50 mM Tris-HCl, pH7.4, 150 mM NaCl, 1 mM EDTA, 1% Triton X-100, proteinase inhibitors). Cell lysates (1–2 mg) were then incubated with 20 μl of anti-FLAG M2 Affinity Gel (Sigma) at 4°C overnight. After washes with the lysis buffer, bound proteins were eluted with 30 μl of 3 × FLAG peptide (150 μg/ml) at 4°C overnight, and subjected to western blotting. For detection endogenous ATF3-p300 interaction, HEK293T cells were lysed in RIPA buffer containing 100 mM NaCl, and lysates (2 mg) were then incubated with 1 μg of p300 antibody or normal IgG for western blotting. GST-pulldown assays were performed essentially as described previously (Cui et al., 2015). Briefly, 1 μg of GST or GST-fusion proteins immobilized on 20 μl of glutathione agarose (Sigma) were incubated with of *in vitro*-translated (5 μl) or recombinant (50 ng) proteins in a buffer containing 20 mM Tri-HCl, pH8.0, 100 mM NaCl, 2 mM EDTA, 2 mM DTT, 5% glycerol and 0.4% NP-40 at 4°C overnight. After extensive washes with a similar buffer containing 150 mM NaCl, bound proteins were eluted by boiling in 20 μl of SDS loading buffer, and subjected to western blotting.

Chromatin immunoprecipitation (ChIP)—ChIP assays were performed following a protocol described previously (Wang et al., 2020; Zhao et al., 2016b). Briefly, cells (10^7) were treated with 1% formaldehyde for 10 min followed by 0.125 M glycine for 5 min at room temperature. After trypsinized and resuspended in 10 mL of Solution I (10 mM HEPES-KOH, pH7.5, 10 mM EDTA, 0.5 mM EGTA, and 0.75% Triton X-100) at 4°C for 10 min, cells were treated with 10 mL of Solution II (10 mM HEPES-KOH, pH7.5, 200 mM NaCl, 1 mM EDTA, and 0.5 mM EGTA) at 4°C for 10 min, and subsequently lysed in cold FA lysis buffere (50 mM HEPES-KOH, pH7.5, 140 mM NaCl, 1 mM EDTA, 1%

Triton X-100, 0.1% sodium deoxycholate, and proteinase inhibitor cocktail). The chromatin were then sheared by sonication using Bioruptor to an average fragment size of 500 bp, followed by incubated with 2 μg of the antibody (ATF3, sc-188X; p300, sc-584; H3K27ac antibody, ab4729) at 4°C overnight. Antibody-bound chromatin was precipitated with 30 μl of ssDNA-protein A agarose at 4°C for 2 h, and subjected to sequential washes with Buffer I (50 mM Tris-HCl, pH8.0, 150 mM NaCl, 1% SDS, 0.5% sodium deoxycholate, 1% NP 40, and 1mM EDTA), Buffer II (buffer I containing 500 mM NaCl), Buffer III (50 mM Tris-HCl, pH8.0, 250 mM LiCl, 0.5% sodium deoxycholate, 1% NP 40, and 1mM EDTA), and TE buffer (50 mM Tris-HCl, pH8.0, and 1 mM EDTA). Bound chromatin was then eluted with 0.3 mL of Elution buffer (50 mM Tris-HCl, pH8.0, 1% SDS, and 1 mM EDTA). After reversal of crosslinking and treatments with RNase A and Proteinase K, DNA was purified by phenol extraction and ethanol precipitation, and subjected to qPCR. The PCR primers are listed in Table S4.

Reporter assays—To generate the PHGDH-enhancer-reporter (en-MiniP) plasmid, the *PHGDH* enhancer fragment (250 bp) was first amplified from genomic DNA by PCR using a forward primer (5′-gtggtaccCGATTCTAGCCTGCCTTGG-3′) and a reverse primer (5′-gaaaagcttGAGGCTAAATCTGGACCCCA-3′), and ligated to the pGL4.29[luc2P/Cre/Hygro] vector (Promega) linearized with KpnI and HindIII (the 3 × CRE sites in the latter plasmid were removed). The linearized vector was also self-ligated to generate the control MiniP reporter. For reporter assays, PC3 cells (1×10^5) cultured in 24-well plates were transfected with 1 ng of pRL-CMV together with 50 ng of en-MiniP, or MiniP, with or without 800 ng of pcDNA3, ATF3, or ATF4 plasmid for 2 days, and then lysed for dual luciferase assays (Promega) following the manufacturer's protocol (Wang et al., 2012, 2020).

RNA-seq assays—RPE cells cultured in the serine-deprived medium or the completed medium for 8 h were lysed followed by RNA extraction using the RNeasy Min Kit (QIAGEN). 0.8 to 1 μg of total RNA samples with a RNA integrity number > 5 were processed for cDNA library preparations using the TruSeq Stranded Total RNA Ribo-zero kit (Illumina) following the manufacturer's protocol. The libraries were then pooled and run on a Hiseq 2500 sequencing system using a 50-cycle paired-end protocol. BCL files generated by sequencing were converted to FASTQ files for the downstream analysis. Reads passed the quality control were aligned to the reference genome through Tuxedo Suite starting with TopHat aligner. The generated BAM files in a comparative setup were imported to the Cufflinks and Cuffdiff tools for outputting differentially-expressed genes with log2 fold changes. Heatmaps were prepared with Morpheus. The unprocessed RNA-seq data can be accessed from GEO (GSE164850).

Stable isotope flux analysis—HCT116 cells (~50% confluence) were washed with PBS, and cultured in HEPES buffered Krebs-Ringer solution supplemented with 25 mM [U-^{13}C]-D-glucose, 10% dialysed FBS, 2 × MEM amino acids, 2 × Vitamin Solution and 4 mM L-glutamine, with or without 0.4 mM serine and glycine, for 24 h. Cells were washed with PBS and metabolites extracted using 1 mL of acetonitrile: isopropanol:water (3:3:2, v/v/v) mixture. The extraction solvent was degassed and pre-chilled at −20°C.

Samples were homogenized using Geno/Grinder 2010 (SPEX SamplePrep) at 1500 rpm for 30 s, then shaken at 4°C for 5 min and centrifuged for 2 minutes at 14,000 r*cf.* 450 μL supernatant was transferred to a new tube and dried down using Centrivap cold trap concentrator (Labconco). 10 μL of methoxyamine hydrochloride in pyridine (40 mg/mL) was added to dried sample and shaken at 30°C for 1.5 hours for methoximation. 90 μL of N-tert-Butyldimethylsilyl-N-methyltrifluoroacetamide (MTBSTFA, Sigma-Aldrich) was used for tertbutylsilylation. C8–C30 fatty acid methyl esters (FAMEs) were added to MTBSTFA as internal standards for retention time correction. Samples were shaken at 37°C for 30 min for TMS or shaken at 80°C for 30 min for TBS and then ready for injection. Gas chromatography-Quadrupole-time of flight mass spectrometry (GC-Q-TOF MS) was used for Stable Isotope enrichment. Rtx-5Sil MS column (30 m length, 0.25 mm i.d, 0.25 μM 95% dimethyl 5% diphenyl polysiloxane film) with an additional 10 m guard column was installed on Agilent 7890 GC (Agilent Technologies). 99.9999% pure Helium gas was used as a mobile phase with a flow rate of 1mL/min. GC temperature was held at 50°C for 1 min, ramped at 20°C/min to 330°C and then held for 5 min. Electron ionization at −70eV was employed on a Agilent 7250 Quadrupole time of flight mass spectrometer (Agilent Technologies) with ion source temperature at 250°C and detector voltage at 1850V. Mass spectra were acquired at an acquisition rate of 5 spectra/s, with a scan range of 85–900 Da. Agilent MassHunter Quantitative Analysis software B.10.00 (Agilent Technologies) was used for post data processing. Peaks with a minimal signal-to-noise ratio of 10 were used for data analysis. Relative abundance of mass isotopomers of each metabolite was calculated by MassHunter. Isotope ratio was further calculated using an abundance of labeled ion divided by an abundance of unlabeled ion. The raw data is available at the NIH Common Funds National Metabolomics Data Repository (NMDR) website, the metabolomics Workbench, where the study has been assigned Project ID # PR001203. The data can be accessed directly via https://doi.org/10.21228/M86Q68.

Xenograft experiments and immunohistochemical (IHC) staining—Animal experiments were carried out according to a protocol approved by the Institutional Committee of Animal Care and Use (ICACU) of the Augusta University. Male athymic nude mice were purchased from Envigo, and housed in a pathogen-free, barrier facility. The mice were fed with a diet free of serine and glycine (5BJX, TestDiet), or a control normal diet (5CC7, TestDiet), two days before the experiments, and were continuously fed with these diets until the end of the experiments. For tumor implantations, HCT116 cells (5×10^6) suspended in PBS were mixed with Matrigel (1:1) and injected into the flanks of nude mice. Tumors were measured every other day with a caliper until the volume of the largest tumor reached ~2,000 mm^3, and then the mice were sacrificed. Tumors were subsequently dissected, weighed, and fixed in 10% of formalin for paraffin embedding. For IHC staining, tumor sections were stained with the Ki67 antibody (ab15580, 1:600, Abcam) using the DAB Kit (Vector) according to the manufacturer's recommendations.

QUANTIFICATION AND STATISTICAL ANALYSIS

Quantification of immunblots was performed using ImageJ. Quantification of immunostaining was performed by counting positively stained cells in different field of view. The data were presented as mean ± SD unless indicated otherwise. Statistical

significance was calculated by two-tailed unpaired Student t test using GraphPad Prism (version 9.0). The number of samples for each experiments is indicated in the respective figure legend.

Supplementary Material

Refer to Web version on PubMed Central for supplementary material.

ACKNOWLEDGMENTS

This work was supported by the NIH grants to C.Y. (R01CA139107 and R01CA240966), H.-F.D. (R01CA190429 and R01CA236890), and X. Long (R01HL122686 and R01HL139794), as well as the US Department of Defense award W81XWH1910587 (to C.Y.). We thank the Georgia Cancer Center Integrated Genomics Core for providing the RNA-seq service and the West Coast Metabolomics Core for the metabolomics assays.

REFERENCES

Bowers EM, Yan G, Mukherjee C, Orry A, Wang L, Holbert MA, Crump NT, Hazzalin CA, Liszczak G, Yuan H, et al. (2010). Virtual ligand screening of the p300/CBP histone acetyltransferase: identification of a selective small molecule inhibitor. Chem. Biol 17, 471–482. [PubMed: 20534345]

Calo E, and Wysocka J (2013). Modification of enhancer chromatin: what, how, and why? Mol. Cell 49, 825–837. [PubMed: 23473601]

Crawford RR, Prescott ET, Sylvester CF, Higdon AN, Shan J, Kilberg MS, and Mungrue IN (2015). Human CHAC1 protein degrades glutathione, and mRNA induction is regulated by the transcription factors ATF4 and ATF3 and a bipartite ATF/CRE regulatory element. J. Biol. Chem 290, 15878–15891. [PubMed: 25931127]

Creyghton MP, Cheng AW, Welstead GG, Kooistra T, Carey BW, Steine EJ, Hanna J, Lodato MA, Frampton GM, Sharp PA, et al. (2010). Histone H3K27ac separates active from poised enhancers and predicts developmental state. Proc. Natl. Acad. Sci. USA 107, 21931–21936. [PubMed: 21106759]

Cui H, Guo M, Xu D, Ding Z-C, Zhou G, Ding H-F, Zhang J, Tang Y, and Yan C (2015). The stress-responsive gene ATF3 regulates the histone acetyltransferase Tip60. Nat. Commun 6, 6752. [PubMed: 25865756]

DeNicola GM, Chen P-H, Mullarky E, Sudderth JA, Hu Z, Wu D, Tang H, Xie Y, Asara JM, Huffman KE, et al. (2015). NRF2 regulates serine biosynthesis in non-small cell lung cancer. Nat. Genet 47, 1475–1481. [PubMed: 26482881]

Di Marcantonio D, Martinez E, Kanefsky JS, Huhn JM, Gabbasov R, Gupta A, Krais JJ, Peri S, Tan Y, Skorski T, et al. (2021). ATF3 coordinates serine and nucleotide metabolism to drive cell cycle progression in acute myeloid leukemia. Mol. Cell 81, 2752–2764.e6. [PubMed: 34081901]

Ding J, Li T, Wang X, Zhao E, Choi JH, Yang L, Zha Y, Dong Z, Huang S, Asara JM, et al. (2013). The histone H3 methyltransferase G9A epigenetically activates the serine-glycine synthesis pathway to sustain cancer cell survival and proliferation. Cell Metab. 18, 896–907. [PubMed: 24315373]

Gargiulo G, Cesaroni M, Serresi M, de Vries N, Hulsman D, Bruggeman SW, Lancini C, and van Lohuizen M (2013). In vivo RNAi screen for BMI1 targets identifies TGF-β/BMP-ER stress pathways as key regulators of neural- and malignant glioma-stem cell homeostasis. Cancer Cell 23, 660–676. [PubMed: 23680149]

Gilchrist M, Thorsson V, Li B, Rust AG, Korb M, Roach JC, Kennedy K, Hai T, Bolouri H, and Aderem A (2006). Systems biology approaches identify ATF3 as a negative regulator of Toll-like receptor 4. Nature 441, 173–178. [PubMed: 16688168]

Hackl C, Lang SA, Moser C, Mori A, Fichtner-Feigl S, Hellerbrand C, Dietmeier W, Schlitt HJ, Geissler EK, and Stoeltzing O (2010). Activating transcription factor-3 (ATF3) functions as a tumor suppressor in colon cancer and is up-regulated upon heat-shock protein 90 (Hsp90) inhibition. BMC Cancer 10, 668. [PubMed: 21129190]

Hai T, and Hartman MG (2001). The molecular biology and nomenclature of the activating transcription factor/cAMP responsive element binding family of transcription factors: activating transcription factor proteins and homeostasis. Gene 273, 1–11. [PubMed: 11483355]

Hai T, Wolfgang CD, Marsee DK, Allen AE, and Sivaprasad U (1999). ATF3 and stress responses. Gene Expr. 7, 321–335. [PubMed: 10440233]

Jan Y-H, Tsai H-Y, Yang C-J, Huang M-S, Yang Y-F, Lai T-C, Lee C-H, Jeng Y-M, Huang C-Y, Su J-L, et al. (2012). Adenylate kinase-4 is a marker of poor clinical outcomes that promotes metastasis of lung cancer by downregulating the transcription factor ATF3. Cancer Res. 72, 5119–5129. [PubMed: 23002211]

Jiang H-Y, Wek SA, McGrath BC, Lu D, Hai T, Harding HP, Wang X, Ron D, Cavener DR, and Wek RC (2004). Activating transcription factor 3 is integral to the eukaryotic initiation factor 2 kinase stress response. Mol. Cell. Biol 24, 1365–1377. [PubMed: 14729979]

Kilberg MS, Shan J, and Su N (2009). ATF4-dependent transcription mediates signaling of amino acid limitation. Trends Endocrinol. Metab 20, 436–443. [PubMed: 19800252]

Kim J-S, Bonifant C, Bunz F, Lane WS, and Waldman T (2008). Epitope tagging of endogenous genes in diverse human cell lines. Nucleic Acid. Res 36, e127. [PubMed: 18784188]

Labuschagne CF, van den Broek NJF, Mackay GM, Vousden KH, and Maddocks ODK (2014). Serine, but not glycine, supports one-carbon metabolism and proliferation of cancer cells. Cell Rep. 7, 1248–1258. [PubMed: 24813884]

Lasko LM, Jakob CG, Edalji RP, Qiu W, Montgomery D, Digiammarino EL, Hansen TM, Risi RM, Frey R, Manaves V, et al. (2017). Discovery of a selective catalytic p300/CBP inhibitor that targets lineage-specific tumours. Nature 550, 128–132. [PubMed: 28953875]

Lassot I, Estrabaud E, Emiliani S, Benkirane M, Benarous R, and Margottin-Goguet F (2005). p300 modulates ATF4 stability and transcriptional activity independently of its acetyltransferase domain. J. Biol. Chem 280, 41537–41545. [PubMed: 16219772]

Lee SH, Krisanapun C, and Baek SJ (2010). NSAID-activated gene-1 as a molecular target for capsaicin-induced apoptosis through a novel molecular mechanism involving GSK3beta, C/EBPbeta and ATF3. Carcinogenesis 31, 719–728. [PubMed: 20110283]

Li AM, and Ye J (2020). The PHGDH enigma: do cancer cells only need serine or also a redox modulator? Cancer Lett. 476, 97–105. [PubMed: 32032680]

Li X, Guo M, Cai L, Du T, Liu Y, Ding H-F, Wang H, Zhang J, Chen X, and Yan C (2020). Competitive ubiquitination activates the tumor suppressor p53. Cell Death Differ. 27, 1807–1818. [PubMed: 31796886]

Liu W, Iiizumi-Gairani M, Okuda H, Kobayashi A, Watabe M, Pai SK, Pandey PR, Xing F, Fukuda K, Modur V, et al. (2011). KAI1 gene is engaged in NDRG1 gene-mediated metastasis suppression through the ATF3-NFkappaB complex in human prostate cancer. J. Biol. Chem 286, 18949–18959. [PubMed: 21454613]

Liu J, Zhang C, Wu H, Sun XX, Li Y, Huang S, Yue X, Lu SE, Shen Z, Su X, et al. (2020). Parkin ubiquitinates phosphoglycerate dehydrogenase to suppress serine synthesis and tumor progression. J. Clin. Invest 130, 3253–3269. [PubMed: 32478681]

Locasale JW (2013). Serine, glycine and one-carbon units: cancer metabolism in full circle. Nat. Rev. Cancer 13, 572–583. [PubMed: 23822983]

Maddocks ODK, Berkers CR, Mason SM, Zheng L, Blyth K, Gottlieb E, and Vousden KH (2013). Serine starvation induces stress and p53-dependent metabolic remodelling in cancer cells. Nature 493, 542–546. [PubMed: 23242140]

Masuoka HC, and Townes TM (2002). Targeted disruption of the activating transcription factor 4 gene results in severe fetal anemia in mice. Blood 99, 736–745. [PubMed: 11806972]

Mattaini KR, Sullivan MR, and Vander Heiden MG (2016). The importance of serine metabolism in cancer. J. Cell Biol 214, 249–257. [PubMed: 27458133]

Mo P, Wang H, Lu H, Boyd DD, and Yan C (2010). MDM2 mediates ubiquitination and degradation of activating transcription factor 3. J. Biol. Chem 285, 26908–26915. [PubMed: 20592017]

Ngo B, Kim E, Osorio-Vasquez V, Doll S, Bustraan S, Liang RJ, Luengo A, Davidson SM, Ali A, Ferraro GB, et al. (2020). Limited environmental serine and glycine confer brain metastasis sensitivity to PHGDH inhibition. Cancer Discov. 10, 1352–1373. [PubMed: 32571778]

Nguyen HCB, Adlanmerini M, Hauck AK, and Lazar MA (2020). Dichotomous engagement of HDAC3 activity governs inflammatory responses. Nature 584, 286–290. [PubMed: 32760002]

Ou Y, Wang S-J, Jiang L, Zheng B, and Gu W (2015). p53 protein-mediated regulation of phosphoglycerate dehydrogenase (PHGDH) is crucial for the apoptotic response upon serine starvation. J. Biol. Chem 290, 457–466. [PubMed: 25404730]

Pacold ME, Brimacombe KR, Chan SH, Rohde JM, Lewis CA, Swier LJ, Possemato R, Chen WW, Sullivan LB, Fiske BP, et al. (2016). A PHGDH inhibitor reveals coordination of serine synthesis and one-carbon unit fate. Nat. Chem. Biol 12, 452–458. [PubMed: 27110680]

Pan Y, Chen H, Siu F, and Kilberg MS (2003). Amino acid deprivation and endoplasmic reticulum stress induce expression of multiple activating transcription factor-3 mRNA species that, when overexpressed in HepG2 cells, modulate transcription by the human asparagine synthetase promoter. J. Biol. Chem 278, 38402–38412. [PubMed: 12881527]

Park Y, Reyna-Neyra A, Philippe L, and Thoreen CC (2017). mTORC1 balances cellular amino acid supply with demand for protein synthesis through post-transcriptional control of ATF4. Cell Rep. 19, 1083–1090. [PubMed: 28494858]

Possemato R, Marks KM, Shaul YD, Pacold ME, Kim D, Birsoy K, Sethumadhavan S, Woo HK, Jang HG, Jha AK, et al. (2011). Functional genomics reveal that the serine synthesis pathway is essential in breast cancer. Nature 476, 346–350. [PubMed: 21760589]

Ran FA, Hsu PD, Wright J, Agarwala V, Scott DA, and Zhang F (2013). Genome engineering using the CRISPR-Cas9 system. Nat. Protoc 8, 2281–2308. [PubMed: 24157548]

Riscal R, Schrepfer E, Arena G, Cissé MY, Bellvert F, Heuillet M, Rambow F, Bonneil E, Sabourdy F, Vincent C, et al. (2016). Chromatin-bound MDM2 regulates serine metabolism and redox homeostasis independently of p53. Mol. Cell 62, 890–902. [PubMed: 27264869]

Rodríguez-Martínez JA, Reinke AW, Bhimsaria D, Keating AE, and Ansari AZ (2017). Combinatorial bZIP dimers display complex DNA-binding specificity landscapes. eLife 6, e19272. [PubMed: 28186491]

Sullivan MR, Mattaini KR, Dennstedt EA, Nguyen AA, Sivanand S, Reilly MF, Meeth K, Muir A, Darnell AM, Bosenberg MW, et al. (2019). Increased serine synthesis provides an advantage for tumors arising in tissues where serine levels are limiting. Cell Metab. 29, 1410–1421.e4. [PubMed: 30905671]

Thiaville MM, Dudenhausen EE, Zhong C, Pan Y-X, and Kilberg MS (2008). Deprivation of protein or amino acid induces C/EBPbeta synthesis and binding to amino acid response elements, but its action is not an absolute requirement for enhanced transcription. Biochem. J 410, 473–484. [PubMed: 18052938]

Wang Z, and Yan C (2015). Emerging roles of ATF3 in the suppression of prostate cancer. Mol. Cell. Oncol 3, e1010948. [PubMed: 27308526]

Wang Q, Mora-Jensen H, Weniger MA, Perez-Galan P, Wolford C, Hai T, Ron D, Chen W, Trenkle W, Wiestner A, and Ye Y (2009). ERAD inhibitors integrate ER stress with an epigenetic mechanism to activate BH3-only protein NOXA in cancer cells. Proc. Natl. Acad. Sci. USA 106, 2200–2205. [PubMed: 19164757]

Wang H, Jiang M, Cui H, Chen M, Buttyan R, Hayward SW, Hai T, Wang Z, and Yan C (2012). The stress response mediator ATF3 represses androgen signaling by binding the androgen receptor. Mol. Cell. Biol 32, 3190–3202. [PubMed: 22665497]

Wang F, Marshall CB, and Ikura M (2013). Transcriptional/epigenetic regulator CBP/p300 in tumorigenesis: structural and functional versatility in target recognition. Cell. Mol. Life Sci 70, 3989–4008. [PubMed: 23307074]

Wang Z, Xu D, Ding H-F, Kim J, Zhang J, Hai T, and Yan C (2015). Loss of ATF3 promotes Akt activation and prostate cancer development in a Pten knockout mouse model. Oncogene 34, 4975–4984. [PubMed: 25531328]

Wang Z, Kim J, Teng Y, Ding H-F, Zhang J, Hai T, Cowell JK, and Yan C (2016). Loss of ATF3 promotes hormone-induced prostate carcinogenesis and the emergence of CK5($^{+}$)CK8($^{+}$) epithelial cells. Oncogene 35, 3555–3564. [PubMed: 26522727]

Wang Z, He Y, Deng W, Lang L, Yang H, Jin B, Kolhe R, Ding H-F, Zhang J, Hai T, and Yan C (2018). Atf3 deficiency promotes genome instability and spontaneous tumorigenesis in mice. Oncogene 37, 18–27. [PubMed: 28869597]

Wang L, Liu Y, Du T, Yang H, Lei L, Guo M, Ding HF, Zhang J, Wang H, Chen X, and Yan C (2020). ATF3 promotes erastin-induced ferroptosis by suppressing system Xc. Cell Death Differ. 27, 662–675. [PubMed: 31273299]

Whitmore MM, Iparraguirre A, Kubelka L, Weninger W, Hai T, and Williams BR (2007). Negative regulation of TLR-signaling pathways by activating transcription factor-3. J. Immunol 179, 3622–3630. [PubMed: 17785797]

Wolfgang CD, Chen BP, Martindale JL, Holbrook NJ, and Hai T (1997). gadd153/Chop10, a potential target gene of the transcriptional repressor ATF3. Mol. Cell. Biol 17, 6700–6707. [PubMed: 9343434]

Wolfgang CD, Liang G, Okamoto Y, Allen AE, and Hai T (2000). Transcriptional autorepression of the stress-inducible gene ATF3. J. Biol. Chem 275, 16865–16870. [PubMed: 10748147]

Wolford CC, McConoughey SJ, Jalgaonkar SP, Leon M, Merchant AS, Dominick JL, Yin X, Chang Y, Zmuda EJ, O'Toole SA, et al. (2013). Transcription factor ATF3 links host adaptive response to breast cancer metastasis. J. Clin. Invest 123, 2893–2906. [PubMed: 23921126]

Wortel IMN, van der Meer LT, Kilberg MS, and van Leeuwen FN (2017). Surviving stress: modulation of ATF4-mediated stress responses in normal and malignant cells. Trends Endocrinol. Metab 28, 794–806. [PubMed: 28797581]

Wu X, Nguyen BC, Dziunycz P, Chang S, Brooks Y, Lefort K, Hofbauer GF, and Dotto GP (2010). Opposing roles for calcineurin and ATF3 in squamous skin cancer. Nature 465, 368–372. [PubMed: 20485437]

Xia Y, Ye B, Ding J, Yu Y, Alptekin A, Thangaraju M, Prasad PD, Ding Z-C, Park EJ, Choi J-H, et al. (2019). Metabolic reprogramming by MYCN confers dependence on the serine-glycine-one-carbon biosynthetic pathway. Cancer Res. 79, 3837–3850. [PubMed: 31088832]

Yan C, and Boyd DD (2006). ATF3 regulates the stability of p53: a link to cancer. Cell Cycle 5, 926–929. [PubMed: 16628010]

Yan C, Lu D, Hai T, and Boyd DD (2005). Activating transcription factor 3, a stress sensor, activates p53 by blocking its ubiquitination. EMBO J. 24, 2425–2435. [PubMed: 15933712]

Yang M, and Vousden KH (2016). Serine and one-carbon metabolism in cancer. Nat. Rev. Cancer 16, 650–662. [PubMed: 27634448]

Ye J, Mancuso A, Tong X, Ward PS, Fan J, Rabinowitz JD, and Thompson CB (2012). Pyruvate kinase M2 promotes de novo serine synthesis to sustain mTORC1 activity and cell proliferation. Proc. Natl. Acad. Sci. USA 109, 6904–6909. [PubMed: 22509023]

Yin X, Dewille JW, and Hai T (2008). A potential dichotomous role of ATF3, an adaptive-response gene, in cancer development. Oncogene 27, 2118–2127. [PubMed: 17952119]

Yuan X, Yu L, Li J, Xie G, Rong T, Zhang L, Chen J, Meng Q, Irving AT, Wang D, et al. (2013). ATF3 suppresses metastasis of bladder cancer by regulating gelsolin-mediated remodeling of the actin cytoskeleton. Cancer Res. 73, 3625–3637. [PubMed: 23536558]

Zhao E, Ding J, Xia Y, Liu M, Ye B, Choi J-H, Yan C, Dong Z, Huang S, Zha Y, et al. (2016a). KDM4C and ATF4 cooperate in transcriptional control of amino acid metabolism. Cell Rep. 14, 506–519. [PubMed: 26774480]

Zhao J, Li X, Guo M, Yu J, and Yan C (2016b). The common stress responsive transcription factor ATF3 binds genomic sites enriched with p300 and H3K27ac for transcriptional regulation. BMC Genomics 17, 335. [PubMed: 27146783]

Highlights

- Serine deprivation induces ATF3 via an ATF4-dependent mechanism
- ATF3 in turn binds to ATF4 and regulates its stability
- ATF3 recruits p300 to promote expression of the serine synthesis pathway genes
- ATF3 promotes serine biosynthesis and tumor growth under serine-limiting conditions

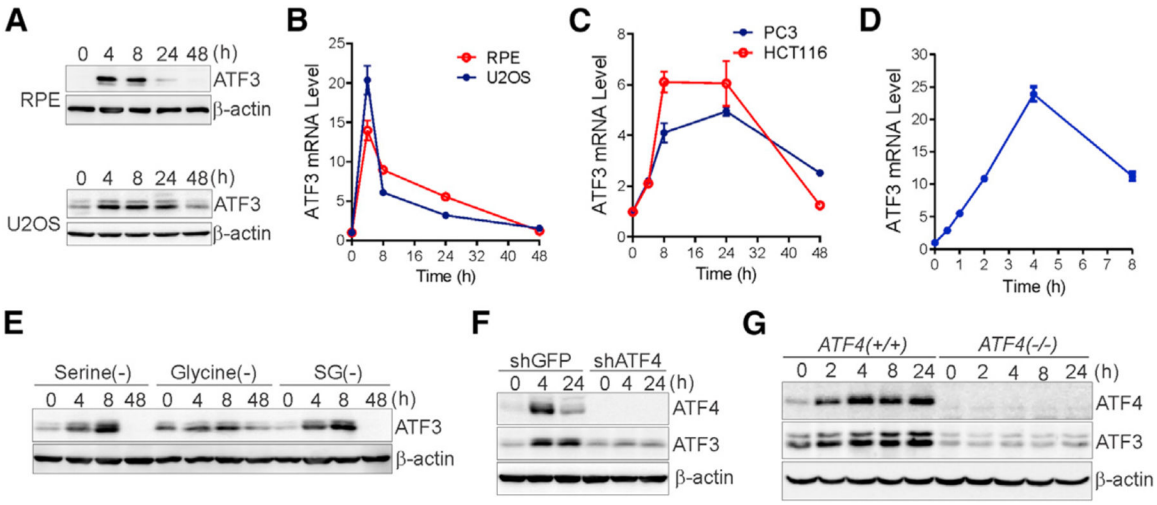

Figure 1. *ATF3* expression is rapidly induced by serine deprivation

(A–C) Indicated cells were cultured in a medium deprived of serine and glycine for 0, 4, 8, 24, and 48 h and harvested for western blotting (A) or qRT-PCR assays (B and C).

(D) RPE cells were cultured in the serine/glycine-deprived medium for 0, 0.5, 1, 2, 4, and 8 h for qRT-PCR assays. The qRT-PCR data are presented as mean ± SD (n = 3). These experiments were repeated at least once.

(E) RPE cells were cultured in a medium deprived of serine (serine(−)), glycine (glycine(−)), or both (SG(−)) for western blotting.

(F) RPE cells were infected with control (shGFP) or lentiviruses expressing *ATF4*-specific shRNA (shATF4) for 3 days and then cultured in the serine/glycine-deprived medium for western blotting.

(G) *ATF4*-wild-type ($ATF4^{+/+}$) or knockout ($ATF4^{-/-}$) HEK293T cells were cultured in the serine/glycine-deprived medium for western blotting.

See also Figure S1.

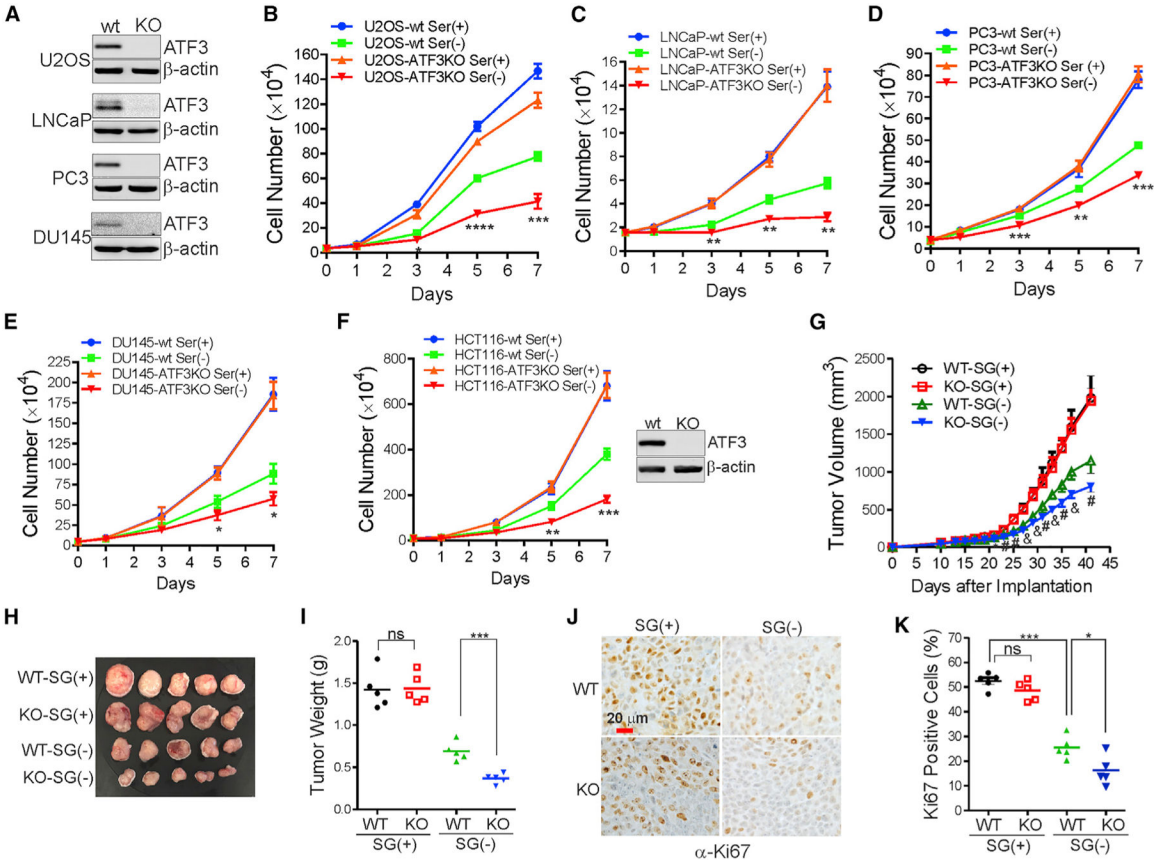

Figure 2. Knockout of *ATF3* expression impairs cancer cell growth under serine-deprived conditions

(A) *ATF3*-knockout (KO) cells developed with CRISPR-Cas9 tools and control wild-type (WT) cells were subjected to western blotting to confirm the loss of *ATF3* expression.

(B–E) Indicated WT or ATF3KO cells were cultured in the serine/glycine-deprived (Ser(−)) or the complete (Ser(+)) medium for different days. Cell numbers were counted, and growth curves were plotted. *p < 0.05; **p < 0.01; ***p < 0.001; ****p < 0.0001; Student's t test; ATF3 KO compared to WT in the absence of serine (Ser(−)); n = 3 (biological replicates).

(F) ATF3KO HCT116 cells developed with an AAV-based precise genome-editing technology and control WT cells were cultured in the serine/glycine-deprived (Ser(−)) or the complete (Ser(+)) medium for different days. The inset shows western blotting results that confirm the loss of *ATF3* expression in the KO cells. **p < 0.01; ***p < 0.001; Student's t test; ATF3 KO compared to WT in the absence of serine (Ser(−)); n = 3 (biological replicates).

(G) WT and *ATF3*-KO HCT116 cells were implanted in nude mice (5 mice each group) fed with a diet deprived of serine and glycine (SG(−)) or a normal control diet (SG(+)). Tumor volumes were calculated and presented in the plot. *p < 0.05; #p < 0.01; &p < 0.001; Student's t test.

(H) A representative image of tumors dissected from the nude mice.

(I) Tumor weights were presented in the plot.

(J and K) Tumor sections were stained for Ki67 expression (J), and positive cells were counted (K). *p < 0.05; ***p < 0.001; ns, not significant; Student's t test.

See also Figure S2.

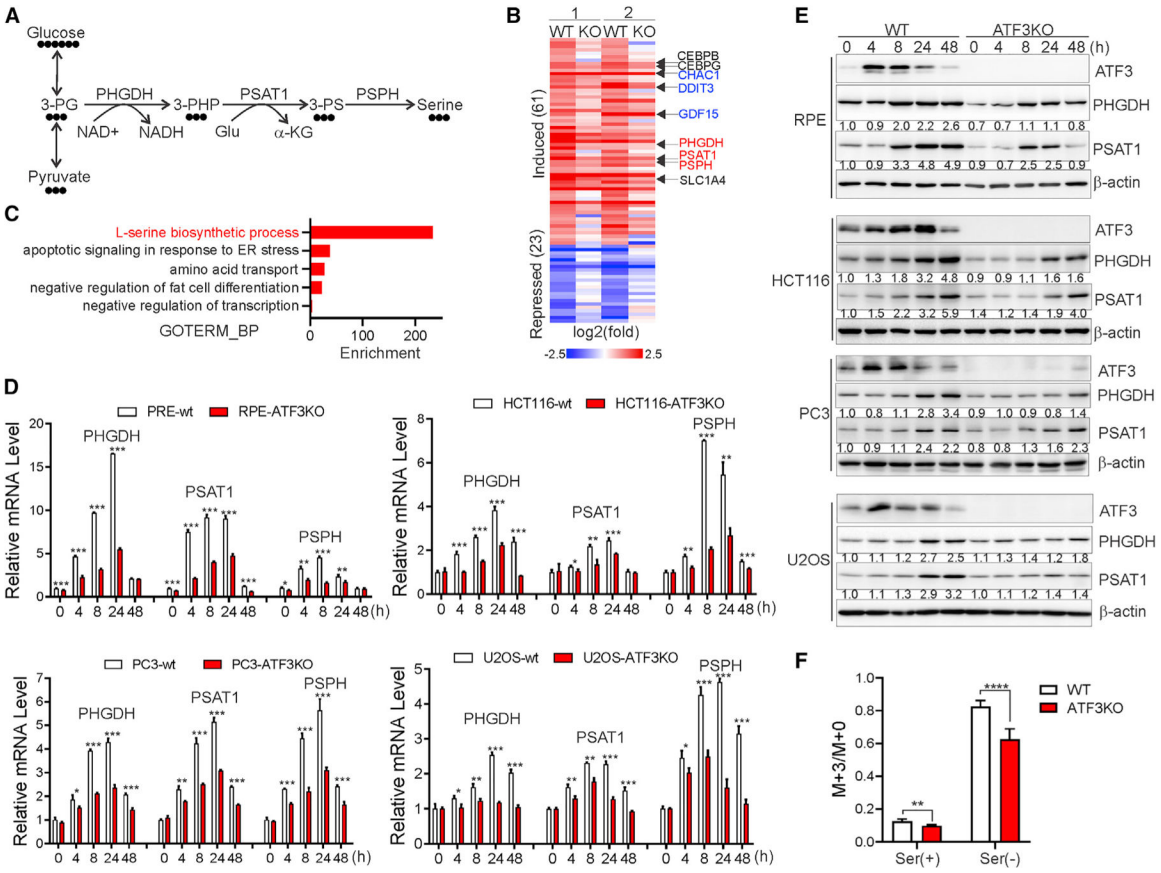

Figure 3. *ATF3* deficiency impairs serine-deprivation-induced expression of serine-synthesis-pathway genes

(A) A diagram shows the serine synthesis pathway. Filled circles represent [^{13}C] atoms derived from [U-^{13}C]-D-glucose.

(B) Heatmap presentation of genes regulated by ATF3 upon serine deprivation. WT or *ATF3*-KO RPE cells cultured in the complete or the serine/glycine-depleted medium for 8 h (2 biological repeats for each sample) were subjected to RNA-seq. Gene expression changes induced by serine deprivation were used to plot the heatmap. The cutoff value (2.5) was chosen to allow for better presentation of differential expression of the majority of genes.

(C) DAVID (Database for Annotation, Visulaization and Integrated Discovery) GO analysis of ATF3-regulated genes upon serine deprivation.

(D) Indicated ATF3KO or control cells were cultured in the serine/glycine-deprived medium for 0, 4, 8, 24, and 48 h for qRT-PCR assays. The data are presented as mean ± SD (n = 3).

(E) Indicated cells cultured in the serine/glycine-deprived medium for 0, 4, 8, 24, and 48 h were subjected to western blotting for *PHGDH* and *PSAT1* expression. The intensities of PHGDH/PSAT1 bands are quantified using ImageJ, normalized to that of β-actin, and indicated under corresponding blots.

(F) WT and *ATF3*-KO HCT116 cells cultured in the medium containing 25 mM of [U-^{13}C]-D-glucose with or without serine/glycine were lysed for metabolomics analyses. L-serine derived from [U-^{13}C]-glucose (M+3) was quantitated and plotted as ratios to unlabeled L-serine (M+0).

n = 6; *p < 0.05; **p < 0.01; ***p < 0.001; ****p < 0.0001; Student's t test. See also Figure S3.

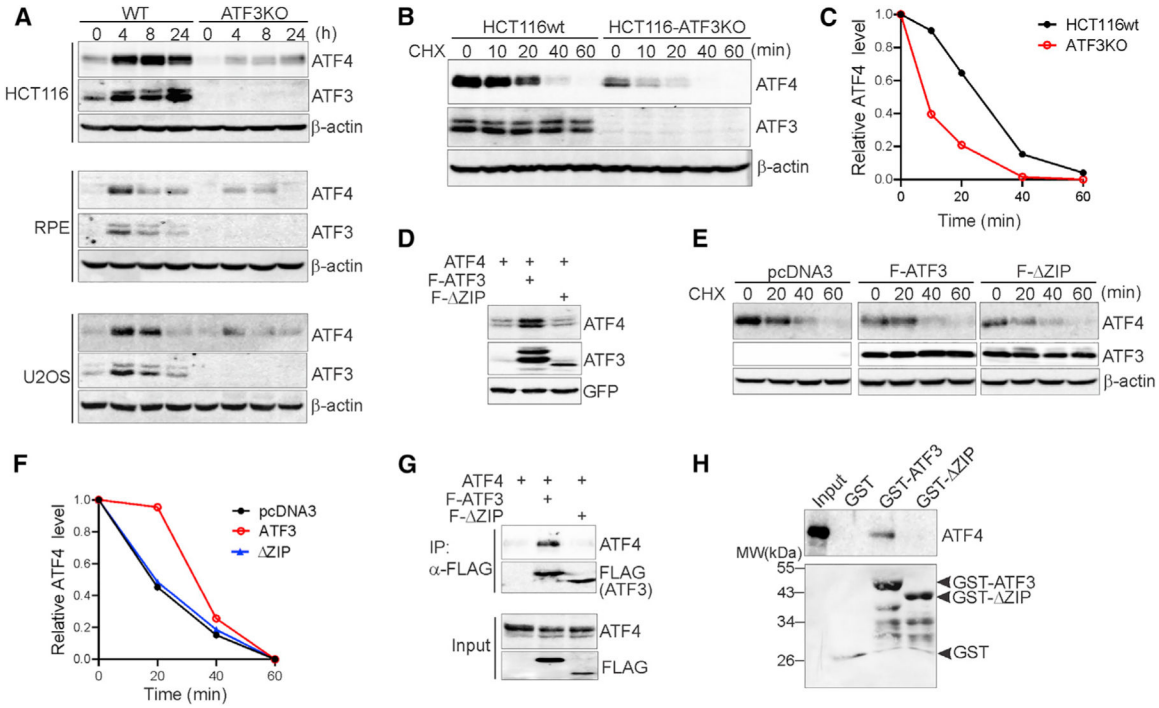

Figure 4. ATF3 binds to ATF4 and increases its stability

(A) Indicated cells cultured in the serine/glycine-deprived medium for 0, 4, 8, and 24 h were subjected to western blotting to detect the ATF4 expression level.

(B and C) WT or ATF3-KO HCT116 cells cultured in the serine/glycine-deprived medium for 8 h were treated with 100 μg/mL of cycloheximide (CHX) for indicated time and then subjected to western blotting. The intensities of the ATF4 bands were quantified and plotted in (C) after normalizing to β-actin.

(D) HEK293T cells were transfected with ATF4 (0.3 μg), EGFP-N1 (0.1 μg), and pcDNA3, FLAG-ATF3, or FLAG-ΔZIP (1.2 μg) for 2 days and then subjected to western blotting after normalizing to the EGFP levels.

(E and F) HEK293FT cells were transfected with ATF4 along with pcDNA3/FLAG-ATF3/FLAG-ΔZIP for 2 days and then treated with 100 μg/mL of CHX for western blotting. Quantification of the ATF4 levels was plotted in (F).

(G) HEK293FT cells transfected with indicated plasmids were subjected to immunoprecipitations using the anti-FLAG M2-affinity agarose.

(H) GST, GST-ATF3, or GST-ΔZIP immobilized onto glutathione agarose was incubated with *in vitro* translated ATF4 for GST-pull-down assays followed by western blotting. The low image shows the blot stained with Ponceau S.

See also Figure S4.

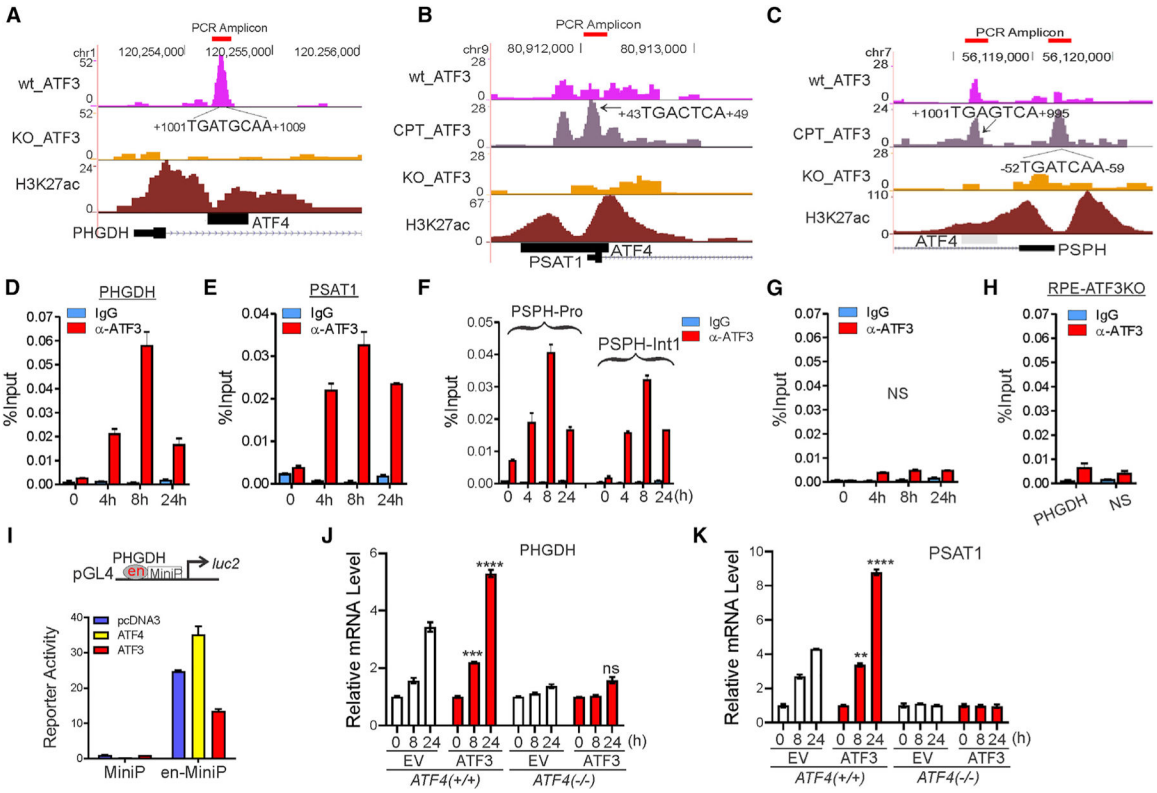

Figure 5. ATF3 binds to the enhancer/promoter regions of SSP genes

(A–C) Genome Browser views of ATF3-binding peaks at regions proximal to transcription start sites of *PHGDH* (A), *PSAT1* (B), or *PSPH* (C). The ChIP-seq data were generated using ATF3-WT and KO HCT116 cells. Data from WT cells treated with camptothecin (CPT, to induce *ATF3* expression) were also presented if basal ATF3 binding was not present or too weak. ATF4 peaks were derived from the ENCODE database, while the enrichment of H3K27ac was also shown.

(D–G) RPE cells cultured in the serine/glycine-deprived medium for 0, 4, 8, and 24 h were subjected to ChIP assays using immunoglobulin G (IgG) or the ATF3 antibody. The amounts of precipitated DNA were quantified by qPCR using primers amplifying the regions indicated in (A), (B), or (C) or a non-specific (NS) region indicated in Figure S5A. The data are presented as mean ± SD (n = 3).

(H) ATF3-KO RPE cells were serine starved for 8 h and subjected to ChIP assays using IgG or the ATF3 antibody. The specific PHGDH and NS region were amplified and quantitated by qPCR.

(I) Cells were co-transfected with a minimal reporter (MiniP), or the PHGDH-enhancer-reporter (en-MiniP), with or without ATF3 or ATF4 for dual luciferase assays. The enhancer-reporter construct was depicted above the plot. n = 3.

(J and K) *ATF4*-WT (*ATF4*$^{+/+}$) and KO (*ATF4*$^{-/-}$) HEK293T cells were infected with lenti-ATF3 (ATF3) or control viruses (EV, empty vector) and subjected to serine starvation for qRT-PCR assays.

The data are presented as mean ± SD (n = 3). **p < 0.01; ****p < 0.0001; Student's t test; compared at the same time point between WT and KO cells. See also Figure S5.

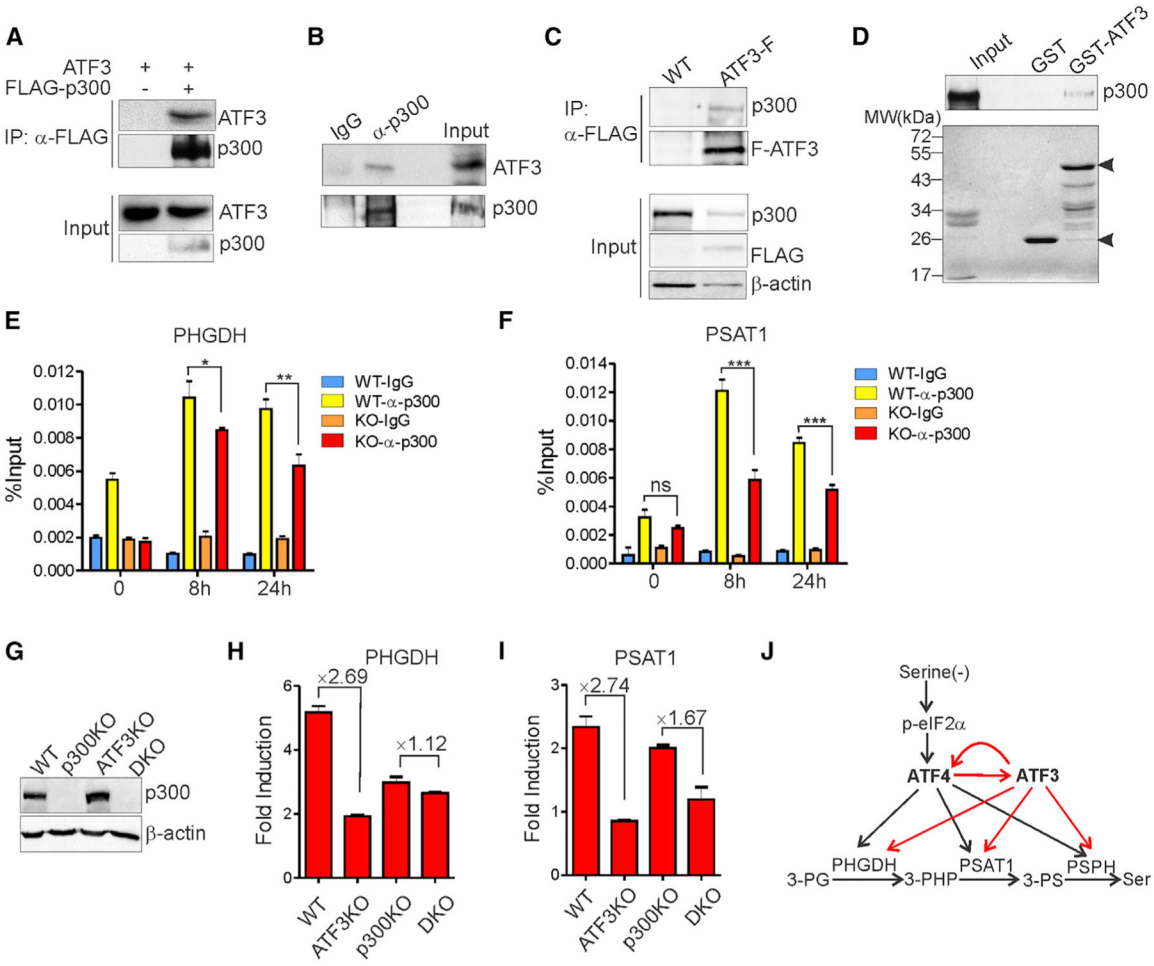

Figure 6. ATF3 binds to p300 and recruits it to SSP genes

(A) ATF3 was co-transfected with or without FLAG-p300 for coIP assays using the FLAG antibody.

(B) 293T cell lysates were incubated with IgG or the p300 antibody for coIP assays.

(C) HCT116 cells (ATF3-F) expressing 3× FLAG-conjugated endogenous ATF3 protein (see Figure S6 for the editing strategy) or its control cells (WT) were lysed and incubated with the FLAG M2 affinity agarose for coIP assays.

(D) Immobilized GST or GST-ATF3 protein was incubated with purified recombinant p300 protein for GST-pull-down assays. Arrows indicate GST or GST-ATF3 protein.

(E and F) WT or *ATF3*-KO RPE cells cultured in the serine/glycine-deprived medium for 0, 8, and 24 h were subjected to ChIP assays using the p300 antibody. The *PHGDH* enhancer (E) and the *PSAT1* promoter region (F) were amplified and quantified by qPCR. The data are presented as mean ± SD (n = 3). *p < 0.05; **p < 0.01; ***p < 0.001; Student's t test.

(G) The CRISPR-Cas9 technology was used to knock out p300 expression (p300KO) from WT and ATF3-KO HCT116 cells. Loss of p300 expression in p300KO and DKO cells was confirmed by western blotting.

(H and I) Indicated HCT116 cells were cultured in normal or the serine/glycine-deprived medium for 24 h and subjected to qRT-PCR to measure the levels of *PHGDH* and *PSAT1*

mRNA. Serine-deprivation-caused fold changes in gene expression were presented. The data are presented as mean ± SD (n = 3).

(J) A model shows that ATF3 induced by ATF4 binds to ATF4 and SSP genes to promote SSP gene expression and serine biosynthesis upon serine deprivation.

See also Figure S6.

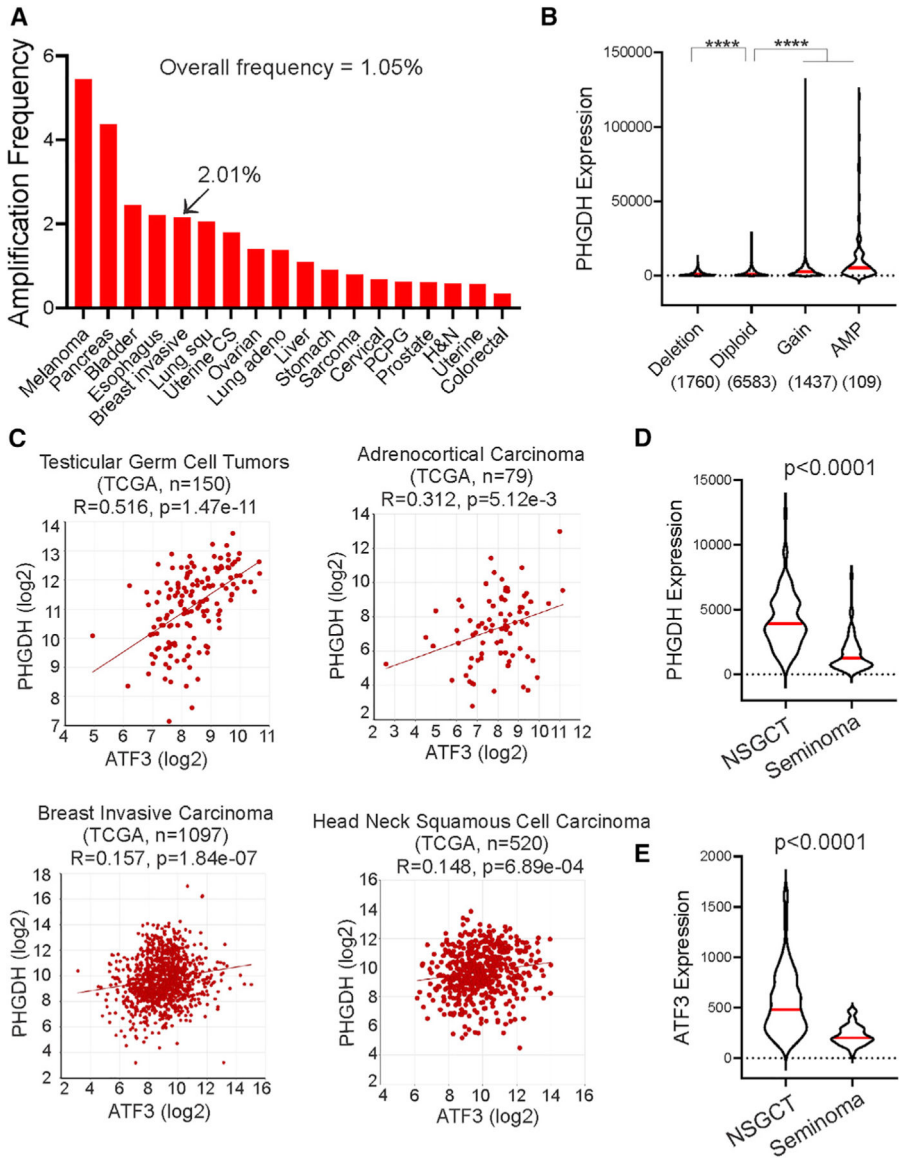

Figure 7. *ATF3* expression positively correlates with *PHGDH* expression in a subset of human cancers

(A) *PHGDH* amplification frequency in different types of cancer. The data were retrieved from cBioPortal (the TCGA PanCancer Atlas Studies).

(B) The *PHGDH* expression level correlates with copy number.

(C) *ATF3* expression positively correlates with *PHGDH* expression in several TCGA patient cohorts ($p < 0.01$). The results were obtained using the R2 Genomics Analysis and Visualization Platform.

(D and E) The expression levels of *PHGDH* (D) and *ATF3* (E) were higher in NSGCTs than that in seminoma.

See also Figure S7.

KEY RESOURCES TABLE

REAGENT or RESOURCE	SOURCE	IDENTIFIER
Antibodies		
ATF3	Santa Cruz	cat#sc-188X; RRID: AB_2258513
ATF3	Cell Signaling	cat#33593; RRID: AB_2799039
ATF4	Cell Signaling	cat#11815; RRID: AB_2616025
p300	Santa Cruz	cat#sc-584; RRID: AB_2293429
p300	Cell Signaling	cat#54062; RRID: AB_2799450
p53	Santa Cruz	cat#sc-126; RRID: AB_628082
PHGDH	Sigma-Aldrich	cat#HPA021241; RRID: AB_1855299
beta-actin	Sigma-Aldrich	cat#A2228; RRID: AB_476697
PSAT1	Novus Biologicals	cat#21020002; RRID: AB_2172599
Ki67	Abcam	cat#ab15580; RRID: AB_443209
H3K27ac	Abcam	Cat#ab4729; RRID: AB_2118291
Chemicals, peptides, and recombinant proteins		
D-glucose (U-^{13}C6)	Cambridge Isotope Laboratories	cat#CLM-1396
L-serine	Sigma-Aldrich	cat#S4500
glycine	Sigma-Aldrich	cat#G7126
Krebs-Ringer solution, HEPES-buffered	Fisher Scientific	cat#AAJ67795AP
MEM Amino Acid solution	Fisher Scientific	cat#11130051
MEM Vitamin Solution	Fisher Scientific	cat#11120-052
L-glutamine	Fisher Scientific	cat#SH3003401
P300	ProteinOne	cat#P2004-01
Glutathione agarose	Sigma-Aldrich	cat#G4510
Anti-FLAG M2 Affinity Gel	Sigma-Aldrich	cat#A2220
Protein A Agarose/Salmon Sperm DNA	Milipore-Sigma	Cat#16-157
3 × FLAG peptide	Sigma-Aldrich	cat#F4799
Critical commercial assays		
RNeasy Mini Kit	QIAGEN	cat#74104
iScript Adv cDNA synthesis Kit	Biorad	cat#1725038
2 × SYBR Green qPCR Master Mix	BiMaker	cat#B21203
TruSeq Stranded Total RNA Libray Prep	Illumina	cat#20020596
DAB Substrate Kit	Vector Laboratories	cat#SK-4100
TNT Quick Coupled Transcription/Translation System	Promega	cat#L1170
Dual-Luciferase Reporter Assay System	Promega	Cat#E1910
Deposited data		
RNA-seq data	This study	GEO GSE164850
Metabolomics data	This study	NMDR PR001203
ChIP-seq data	(Zhao et al.,2016b)	GEO GSE74363
Experimental models: cell lines		
LNCaP	ATCC	CRL-1740

REAGENT or RESOURCE	SOURCE	IDENTIFIER
PC3	ATCC	CRL-1435
DU145	ATCC	HTB-81
HCT116-wt	ATCC	CCL-247
U2OS	ATCC	HTB-96
HEK293T	ATCC	CRL-3216
hTERT-RPE1	(Kim et al., 2008)	N/A
HCT116-ATF3(−/−)	(Zhao et al., 2016b)	N/A
HEK293T-ATF4(−/−)	Park et al., 2017	N/A
Experimental models: organisms/strains		
athymic nude mouse, Hsd:Athymic Nude-Foxn1^{nu}	Envigo	cat#069
Oligonucleotides		
PCR primers, see Table S4	This study	N/A
Recombinant DNA		
pGL4.29[luc2P/Cre/hygro]	Promega	cat#E8471
pSpCas9(BB)-2A-puro (pX459)	Addgene	Cat#62988
pX459-sgATF3	This study	N/A
pX459-sgp300	This study	N/A
PGEX-3X-ATF3 (GST-ATF3)	Yan et al., 2005	N/A
pGEX-3X-ΔZip (GST-ΔZip)	Yan et al., 2005	N/A
Software and algorithms		
Prism GraphPad 9	GraphPad	N/A
ImageJ	NIH	N/A
MassHunter Quantitative Analysis	Agilent	N/A